



# Technical Note

## ■ An Analysis of Blood Processing Methods to Prepare Samples for GeneChip® Expression Profiling

Several different blood processing techniques are currently available to isolate blood cells for RNA purification. These approaches may affect gene expression profiles differently. In order to understand how they impact the sensitivity and variability of expression profiling results with GeneChip® arrays, a systematic analysis was conducted to survey some commonly used techniques. The effects of different processing temperatures and prolonged storage of blood prior to processing were also examined.

Differences in gene expression results were observed using different blood processing methods and are presented in this Technical Note. In addition, incubation of blood overnight before processing was shown to alter the gene expression profiles drastically. Based on these findings, the practical considerations of choosing a blood technique are discussed. Researchers are encouraged to carefully assess which fraction of blood cells is relevant to their research, their microarray assay sensitivity/variability requirements, and the equipment and resource constraints at the site of blood draw in order to make more knowledgeable decisions in selecting blood RNA isolation techniques most suitable for their research needs.

### Introduction

Peripheral blood has been an attractive tissue type for biomedical and clinical research, because of its critical role in immune response and metabolism in humans and animal studies, as well as the simplicity and ease of sample collection. Blood is used in biomarker discovery and development of diagnostics in hematological diseases and is also being explored to discover surrogate markers in a wide range of non-hematological disorders. To this end, it is critical that the methods of RNA extraction from blood are effective and efficient.

Many different techniques are used to separate fractions of blood cells prior to RNA isolation, but the impact of these different approaches on genome-wide

expression profiling of blood using high-density microarrays has not been well characterized with respect to sensitivity and variability. This Technical Note reports a study which compared commonly used blood isolation and separation protocols, including the PAXgene™ Blood RNA Isolation System, QIAamp® RNA Blood Mini Kits, the Ficoll-Hypaque method (referred to as Ficoll in this Technical Note for simplicity), and BD Vacutainer™-CPT™ Sodium Citrate Tubes. In addition to comparing the gene expression results of different blood processing protocols obtained on the Affymetrix GeneChip® arrays, some variations on the protocols were carried out, such as time delays from blood draw to processing and changes in temperature.

Cell Type	Approximate Number in 1 $\mu$ L of Blood (Fauci <i>et al</i> )	Representative Blood Cell Isolation/Separation Techniques			
		<i>Whole blood:</i> • PAXgene	<i>Erythrocyte lysis:</i> • QIAamp	<i>PBMC:</i> • Ficoll • BD-CPT	<i>Specific cells*:</i> • Positive selection • Negative selection
Red blood cells	4,15 – 4,9 million	✓			Any specific subset of cells
Platelets	130,000 – 400,000	✓	✓		
White blood cells	4,300 – 10,800				
Granulocytes: • Neutrophils • Basophils • Eosinophils	4,500 – 8,300 0 – 20 0 – 700	✓	✓		
Mononuclear cells: • Lymphocytes • Monocytes	1,600 – 4,500 40 – 100	✓	✓	✓	

**Table 1.** Cell types in blood isolated by various separation and fractionation techniques.

\*Not shown in this study.

As shown in Table 1, several techniques are available for working with blood. These methods include isolation of RNA from whole blood, the selective lysis of erythrocytes prior to RNA isolation, purification of peripheral blood mononuclear cells (PBMC), or separation of specific cell populations based on characteristic cell surface antigens. Cell types predominantly isolated by these techniques and their relative representation in blood (approximate number in 1  $\mu$ L of blood) are summarized here.

PBMCs are the most transcriptionally active cells in blood. As a result, most studies conducted thus far on blood in many areas of research – such as immunology, infectious and cardiovascular diseases, cancer and biomarker research – have featured the PBMC fraction. This fraction is conventionally isolated by centrifuging whole blood in a liquid density step gradient. It contains lymphocytes and monocytes while excluding red blood cells and granulocytes (eosinophils, basophils, and neutrophils).

Mature red blood cells do not contain RNA but reticulocytes — immature red blood cells — do contain RNA (rRNA, tRNA, and mRNA). The most predominant transcript category in reticulocytes is globin mRNA. Although reticulocytes represent only 0.5 percent to 2.0 percent of the red blood cells in a healthy individual, their RNA may contribute up to 70 percent of total RNA isolated from whole blood due to the very high number of red blood cells present in blood.

The sensitivity and specificity of microarray data can be improved with finer fractionation to eliminate contaminating cell types, such as reticulocytes. As shown in Table 1, different fractionation techniques generate various degrees of homogeneity of the cell types in which researchers are interested. However, as demonstrated in Table 2, the additional cell separation manipulation may require

Method	Equipment for blood processing before total RNA isolation	Length of procedure before total RNA isolation	Total RNA isolation technique	RNA stabilization
Ficoll	Swinging bucket centrifuge	100 – 150 minutes	TRIzol	No
BD-CPT	Swinging bucket centrifuge	60 – 90 minutes	TRIzol	No
QIAamp	Microcentrifuge	35 – 45 minutes	Column-based purification	No
PAXgene – User developed protocol	N/A	120 minutes	Column-based purification	Yes

**Table 2.** Summary of blood cell fractionation techniques.

immediate processing of blood at the site of blood draw, longer processing time, and additional equipment, all of which may induce *ex vivo* change in expression in certain transcripts.

In order to achieve a balance between the feasibility of performing the additional fractionation of blood cells and the sensitivity and variability requirements of the research, the pros and cons of each technique must be evaluated. Previous studies have been hampered by additional variables associated with individuals, such as gender, age, and health status. In order to minimize these variables, all analyses comparing different techniques were performed in this study on split samples from the same individuals. To also evaluate variables associated with individuals, multiple samples were collected for each method as described in detail in Materials and Methods.

This Technical Note characterizes the impact of different blood separation and isolation techniques on the quality of expression profiling data when used in conjunction with GeneChip microarrays. Direct comparisons of different RNA isolation protocols, as well as various experimental conditions associated with the protocols, are summarized and discussed. The results are presented to help users of GeneChip technology make know-

ledgeable decisions when choosing the most suitable blood and RNA isolation technique for their research purposes.

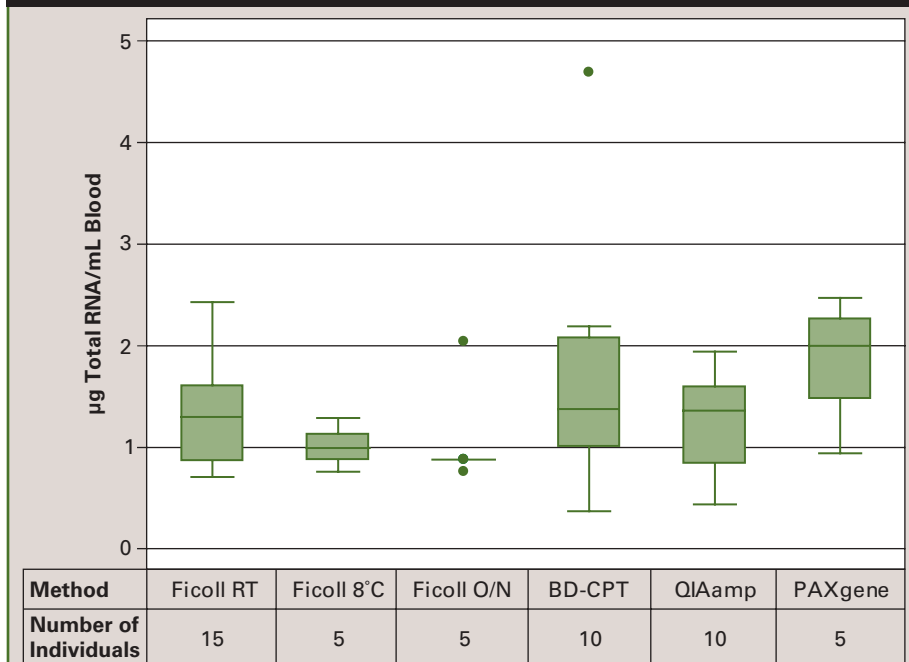
## Results

### TOTAL RNA ISOLATION

Sufficient quantities of high-quality RNA are necessary for expression analysis on microarrays. Therefore, quantity and quality of total RNA isolated from blood are important metrics when deciding which blood isolation technique to use. In order to compare Ficoll, BD-CPT, QIAamp, and PAXgene isolation techniques, RNA was isolated as described in Materials and Methods. Multiple samples were collected for each technique as indicated in Figure 1.

Due to some speculation that the manipulation inherent in Ficoll gradient separation may induce changes in the expression profile due to transcriptional activation of PBMC, some researchers opt to perform the gradient separation at lower temperatures to minimize these changes. In order to determine if the temperature of processing affects the quantity and quality of RNA isolated, the Ficoll technique was performed at two different temperatures, either at room temperature (Ficoll RT), or at 8°C (Ficoll 8°C).

**Figure 1:** Total RNA yield obtained using different blood processing methods. The y-axis shows the total RNA yield and the x-axis shows the technique used for preparation of RNA from blood. The box and whisker plot (Tukey, 1977) represents the interquartile range (between 25% and 75%), and the line within the box denotes the median. The whiskers extend to the last observation before the outliers, which are plotted individually as dots. The table below the figure indicates the number of individuals represented in each method.



Another variable that can occur in RNA isolation from blood is a time delay between blood draw and processing. Published studies have indicated that when blood is drawn at collection centers and shipped overnight at ambient temperatures, there can be a delay of up to 24 hours from the time blood is drawn until

the time it can be processed (de Primo, *et al*, 2003). To evaluate the effect of this time delay, fractionation was performed immediately after blood draw, as well as after storage of blood for 20 to 22 hours (Ficoll O/N).

As shown in Figure 1, reasonable amounts of total RNA were isolated from

all procedures for target labeling for GeneChip expression analysis.

To assess the quality and integrity of the purified total RNA samples, agarose gel electrophoresis was performed on representative samples. As shown in Figure 2, high-quality RNA was obtained from all isolation protocols. In addition, the OD<sub>260/280</sub> ratios for quantitative RNA quality assessment also met the general requirements (1.9 to 2.1) for proceeding to target labeling for GeneChip array analysis.

The fact that high quality RNA was purified from overnight incubation of blood prior to Ficoll centrifugation was not surprising since the Ficoll gradient itself serves as a screen for live cells. Although there may be cell death occurring during the delay, intact RNA was obtained from the isolated cells.

#### TARGET LABELING

To evaluate whether the total RNA samples can be processed efficiently using the standard GeneChip target labeling protocol in conjunction with blood isolation techniques, 5 to 15 µg of total RNA were used to generate labeled cRNA targets. As shown in Figure 3, all methods yielded adequate amounts of cRNA for array hybridization as described in the GeneChip Expression Analysis Technical Manual (available at [www.affymetrix.com](http://www.affymetrix.com)).

**Figure 2:** Integrity of total RNA samples isolated from different blood processing methods. 1 µg of total RNA isolated by different methods was run on agarose gels. The size marker used was the High Range RNA Ladder from MBI Fermentas. The sizes are shown next to the bands. The RNA obtained was of high quality, as observed by the relative intensities of the 28S and 18S ribosomal bands.

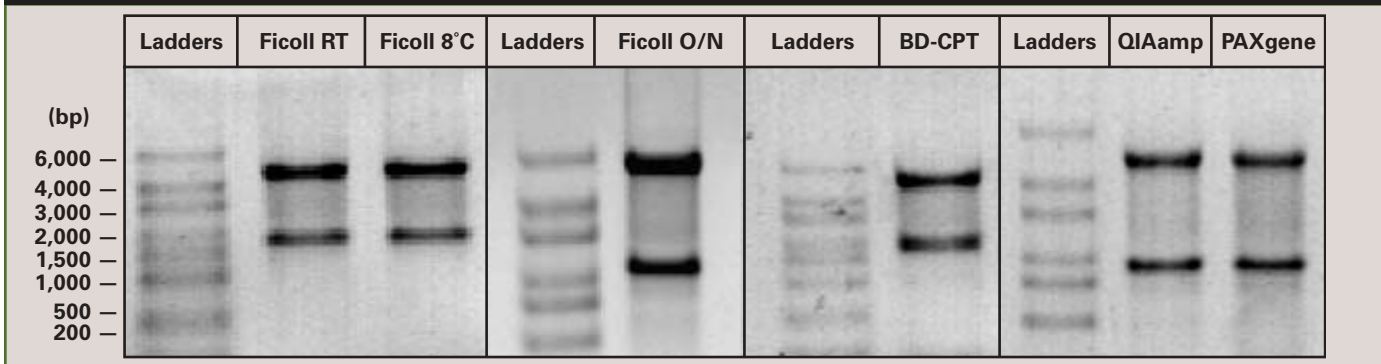
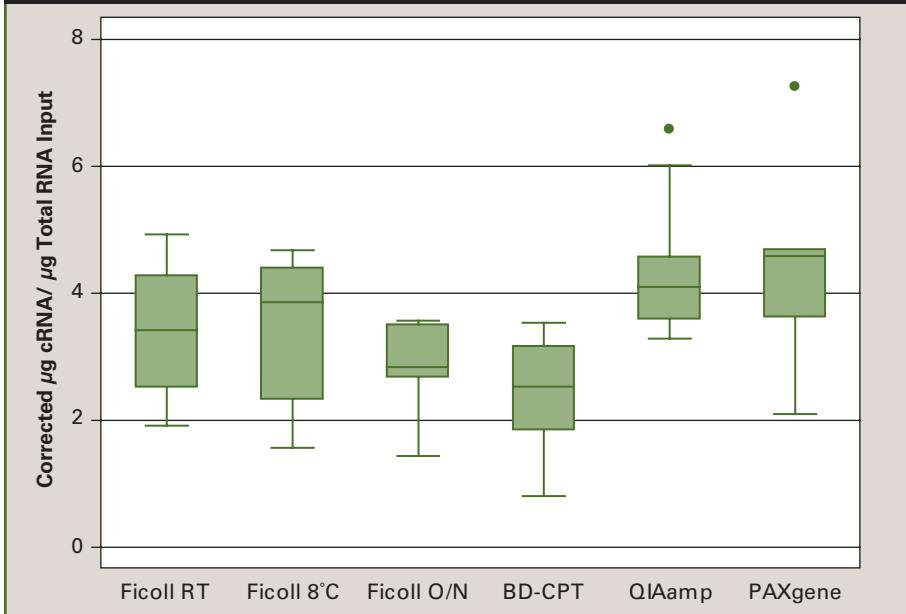


**Figure 3:** Yield of cRNA targets labeled from samples obtained using different blood processing methods. The box and whisker plot (Tukey, 1977) represents the interquartile range (between 25% and 75%), and the line within the box denotes the median. The whiskers extend to the last observation before the outliers which are plotted individually as dots. The cRNA yield is shown on the y-axis as  $\mu\text{g}$  of cRNA obtained per  $\mu\text{g}$  total RNA. The x-axis shows the different techniques used for preparation of RNA from blood.



To assess the length of the cRNA targets, agarose gel electrophoresis was performed on representative samples.

As shown in Figure 4, a typical range of cRNA target lengths (300 bp – 2 kb) was

obtained with Ficoll, BD-CPT tubes, and QIAamp. The Ficoll O/N samples (not shown) also generated cRNA targets comparable to other Ficoll methods. However, with PAXgene, a dominant band is observed

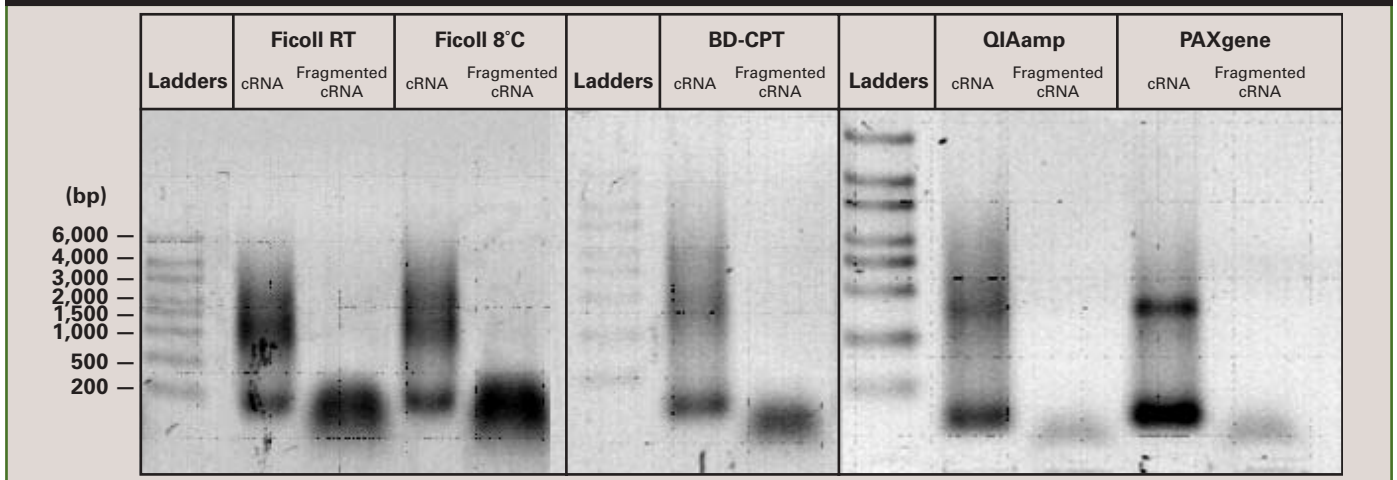
in the 700 bp range (also faintly visible in QIAamp samples) and the relative intensity of the cRNA smear is lower than with other methods. This dominant band is attributed to amplification from globin messages from the red blood cells that are only present in the PAXgene preparations but removed in other methods (Affymetrix, data not shown). The relative reduction in cRNA intensity of the PAXgene samples may result from the competition between the abundant globin messages and the remaining transcripts during amplification and labeling.

#### GENECHIP ARRAY QUALITY ASSESSMENT METRICS

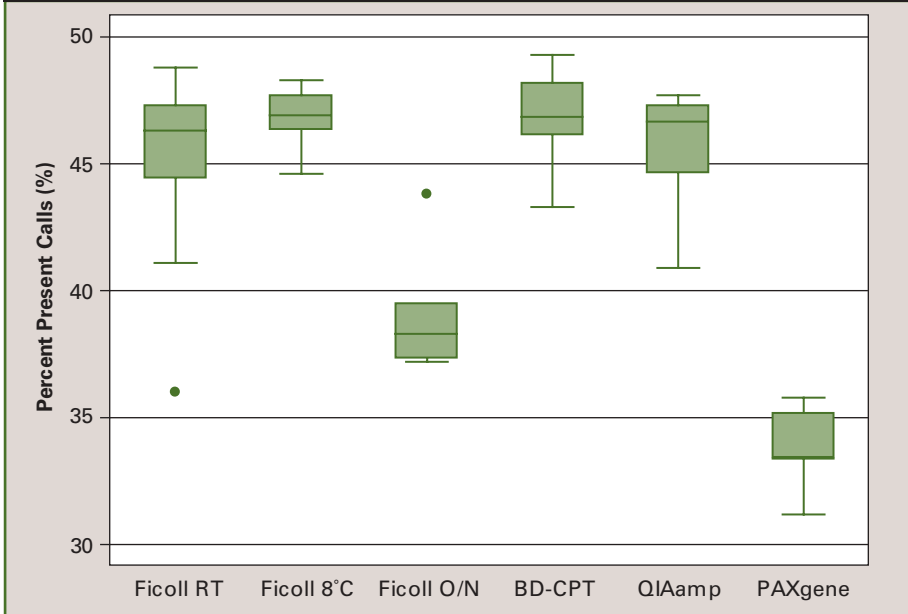
After the labeled cRNA targets were hybridized to Affymetrix GeneChip® Human Genome U133A Arrays, the data were analyzed with Affymetrix® Microarray Suite (MAS) 5.0 software. Percent Present calls, RawQ, and Background were used to measure array data quality. Of these metrics, RawQ and Background were determined to be comparable among all methods.

Figure 5 demonstrates the results obtained with Percent Present calls. Although high-quality total RNA was obtained from all methods, consistently lower Percent Present calls are observed in

**Figure 4:** Labeled cRNA. 1  $\mu\text{g}$  of cRNA was run on agarose gels before and after the fragmentation reaction. The size marker used was the High Range RNA Ladder from MBI Fermentas. The sizes are shown next to the bands.



**Figure 5:** Percent Present calls from arrays hybridized to samples prepared by several techniques. The box and whisker plot (Tukey, 1977) represents the interquartile range (between 25% and 75%), and the line within the box denotes the median. The whiskers extend to the last observation before the outliers which are plotted individually as dots. The y-axis shows Percent Present calls and the x-axis shows the method used.



**IMPACT ON EXPRESSION PROFILES – FICOLL CENTRIFUGATION PROCESSING TEMPERATURE**

For this direct comparison, blood was drawn from each of the five volunteers into citrate tubes. Each blood sample was then split at this stage to be processed by Ficoll centrifugation, either at room temperature or at 8°C. FACS analysis was then conducted on the isolated PBMC fractions to compare the variability and efficiency of the separation methods. The results indicated that there was no significant difference in cell distribution in the PBMC fractions obtained either after processing at room temperature or 8°C (Figure 6). The analysis of T cell subsets (CD4<sup>+</sup>, CD8<sup>+</sup>, CD25<sup>+</sup>, CD69<sup>+</sup>) also did not reveal any difference (not shown).

Total RNA was then isolated from individual PBMC fractions, labeled cRNA targets were generated following the standard GeneChip® Eukaryotic Labeling Assay and hybridized to HG-U133A

the PAXgene and the Ficoll O/N samples. These data indicate that whole blood preparation (PAXgene) or delays between blood draw and processing time (Ficoll O/N) can affect the expression results. The reduced sensitivity seen in the PAXgene experiment may be due to the presence of the dominant band in the amplified cRNA target (Figure 4), contributed by the red blood cells in the whole blood RNA preparation.

GAPDH and Actin 3'/5' ratios were used to assess the extent of RNA sample degradation and the efficiency of the target labeling reaction. With all protocols, both ratios were under 3, indicating that the sample integrity was maintained.

**Figure 6:** FACS analysis of PBMC samples. The major cell subtypes are shown here: CD3<sup>+</sup> T cells, CD19<sup>+</sup> and CD20<sup>+</sup> B cells, CD16<sup>+</sup> and CD56<sup>+</sup> NK cells, and CD14<sup>+</sup> monocytes. Isolation of cells was either performed at room temperature (RT) or at 8°C (8°C). The range (5% to 95%), median and standard deviations are shown.

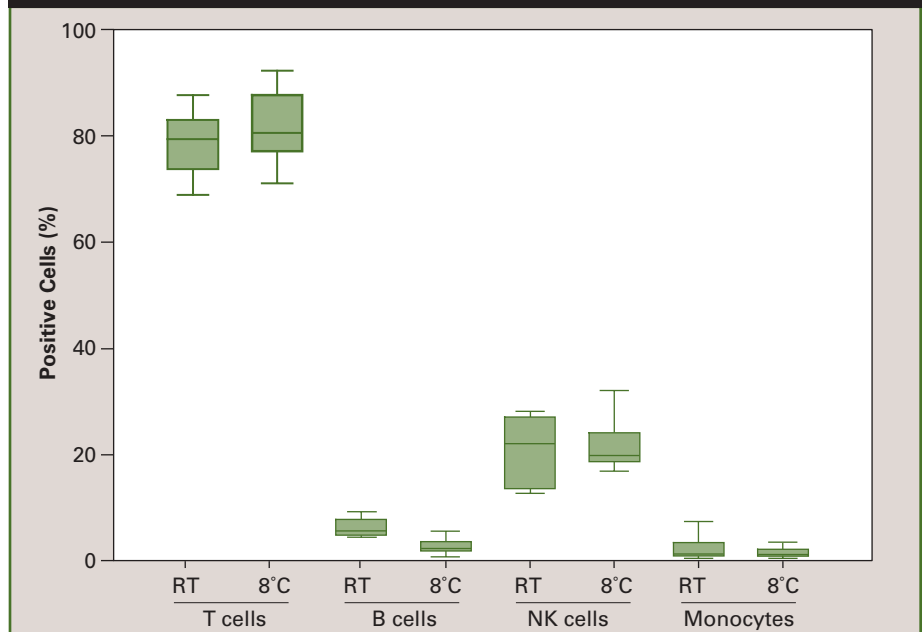
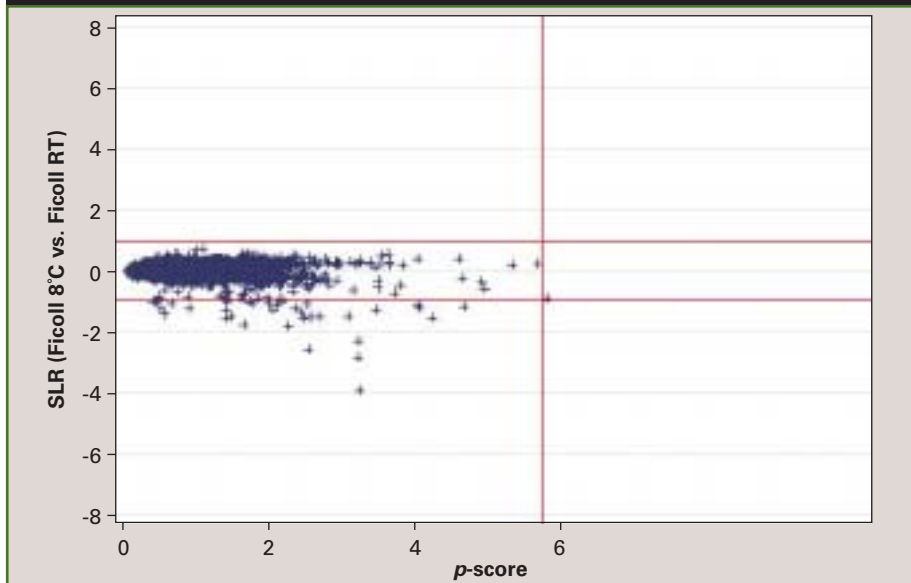


**Figure 7:** Signal Log Ratios (SLR) of samples processed at different temperatures on the Ficoll gradient. The y-axis shows the SLR computed by MAS 5.0, comparing results from processing at 8°C vs. processing at room temperature (baseline for SLR calculation). On the y-axis, 0 represents no change; the two horizontal lines at +1 and -1 represent probe sets that are expressed 2-fold higher or 2-fold lower, respectively. The x-axis shows the *p*-score, defined here as the negative log of the *p*-value from the paired *t*-test. A higher *p*-score indicates higher statistical significance of change. The vertical line represents the Bonferroni 95% significance cutoff. Probe sets to the right of the vertical line signify significant differences between the two methods.



significance of the change for each probe set. As a result, the probe sets that show significant difference in expression based on either criterion can be clearly visualized.

As seen in Figure 7, the majority of probe sets showed less than a two-fold change. Only one probe set demonstrated statistical significance according to the Bonferroni test at the 95% confidence level (see Appendix 2 for description of this probe set). Based on this study, while it is possible that processing at the two different temperatures may induce some change in gene expression, these changes are likely to be subtle or rare.

**IMPACT ON EXPRESSION PROFILES – DELAY IN BLOOD PROCESSING ON FICOLL GRADIENT**

To measure the effect of a time delay from blood draw to processing, blood was drawn from five individuals into citrate tubes. Each blood sample was then split into two and processed either immediately by Ficoll centrifugation, or after storage

arrays. A paired *t*-test was used to identify the genes that showed differential expression between these two methods.

In theory, between two samples, the magnitude of change in expression levels for the same probe set correlates to the statistical significance of change. However, in practice, due to the unpredictable experimental noise and biological variables, the magnitude of change may become disconnected from the statistical significance value of change. In this case, false positives may be selected whenever magnitude of change is the sole criterion. For example, probe sets with a large magnitude of change may not also be significantly changed by statistical criteria.

The results are displayed with a volcano plot (see Figure 7). This type of plot (Russ Wolfinger, SAS) displays both the magnitude of change and the statistical

**Figure 8:** FACS analysis of PBMC samples. The major cell subtypes are shown here: CD3<sup>+</sup> T cells, CD19<sup>+</sup> and CD20<sup>+</sup> B cells, CD16<sup>+</sup> and CD56<sup>+</sup> NK cells, and CD14<sup>+</sup> monocytes. Isolation of cells was performed after immediate isolation of PBMC (ASAP) or after overnight (O/N) storage of blood sample (20-22 hours) and subsequent isolation of PBMC. The range (5% to 95%), median and standard deviations are shown. The asterisk indicates a significant change (*p*<0.05).

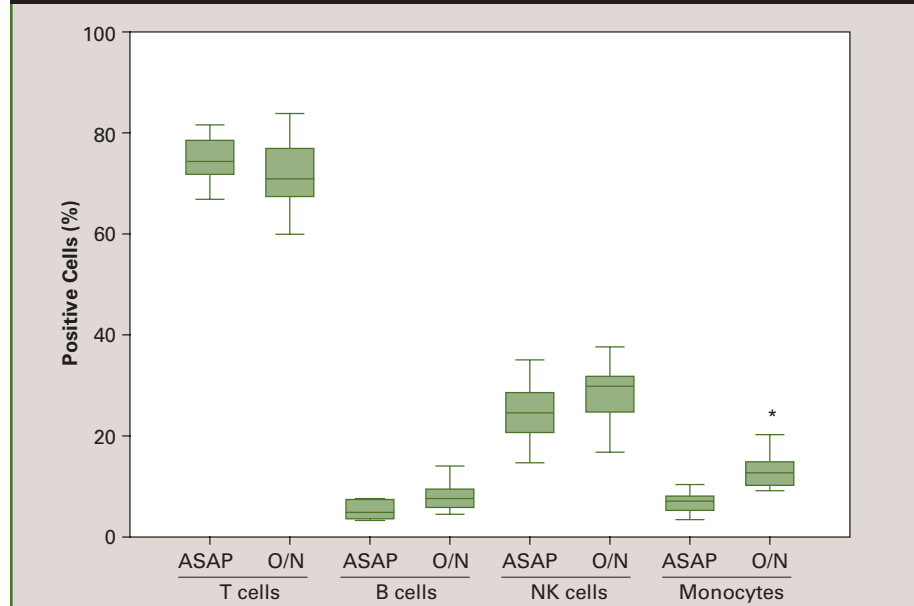
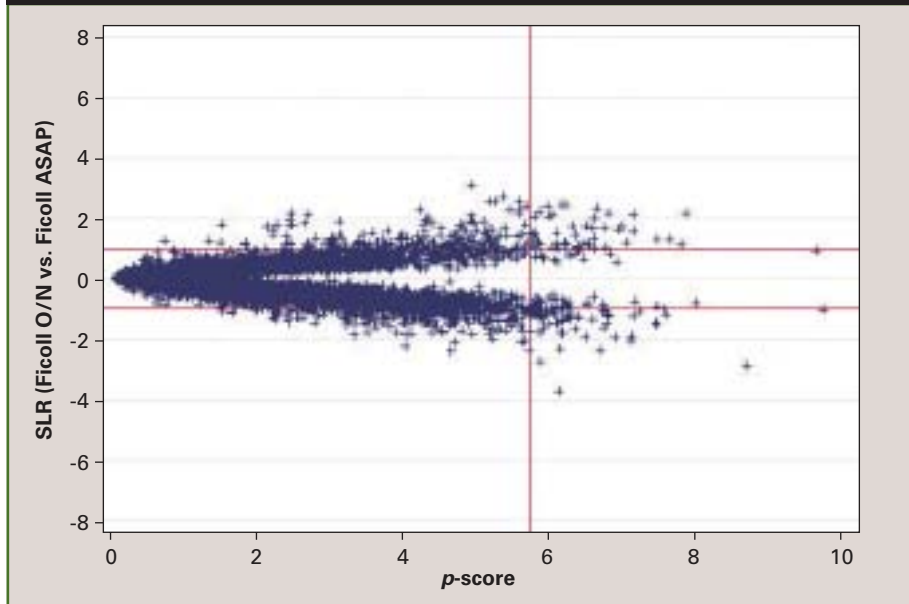


**Figure 9:** Signal Log Ratios (SLR) of samples processed after different delays before Ficoll centrifugation. The y-axis shows the SLR computed by MAS 5.0, comparing results from processing after overnight storage of blood to those prepared immediately (baseline for SLR calculation). On the y-axis, 0 represents the no change line, the two horizontal lines at +1 and -1 represent probe sets that are expressed 2-fold higher or 2-fold lower, respectively. The x-axis shows the  $p$ -score, defined here as the negative log of the  $p$ -value from the paired  $t$ -test. A higher  $p$ -score indicates higher statistical significance of change. The vertical line represents the Bonferroni 95% significance cutoff. Probe sets to the right of the vertical line show significant difference between the two methods.



overnight (20-22 hours) at room temperature. FACS analysis was performed immediately after isolation of PBMC at either time point. The results are shown in Figure 8. Except for a relative increase in the proportion of monocytes, there was no striking difference between PBMC isolated immediately after blood draw and blood stored overnight. The analysis of T cell subsets revealed a slightly greater range in the CD4<sup>+</sup> T cell subset after overnight storage (data not shown). Comparing other T cell subsets (CD8<sup>+</sup>, CD25<sup>+</sup>, CD69<sup>+</sup>) demonstrated no differences between the two approaches.

Total RNA was then isolated from individual PBMC fractions and labeled cRNA was prepared, and hybridized onto HG-U133A arrays. As shown previously, reduced Percent Present Calls were obtained from samples stored overnight (Figure 5). A paired  $t$ -test was performed

to identify probe sets that were expressed differently in each method. The results are plotted in Figure 9.

A comparison of the two processing times used in the Ficoll protocol reveals global changes in the resulting gene expression profiles. 150 probe sets showed significant difference in expression, with 90 expressed at a higher level in the samples that were prepared immediately and 60 probe sets expressed at a higher level in the O/N samples. Preliminary GO analyses of these genes on the NetAffx™ Analysis Center ([www.affymetrix.com](http://www.affymetrix.com)) suggest that genes involved in cellular metabolism are down-regulated after O/N storage. The probe sets are listed in Appendix 3.

As assessed by gel electrophoresis, general RNA degradation was not detected after overnight incubation (Figure 2). The cell composition as observed by FACS analysis is generally comparable (Figure 8).

Further analysis is necessary to better understand the mechanisms for the observed differences in gene expression. Nevertheless, these results clearly demonstrate that prolonged incubation of the blood samples prior to processing significantly alters array results, and may complicate interpretation.

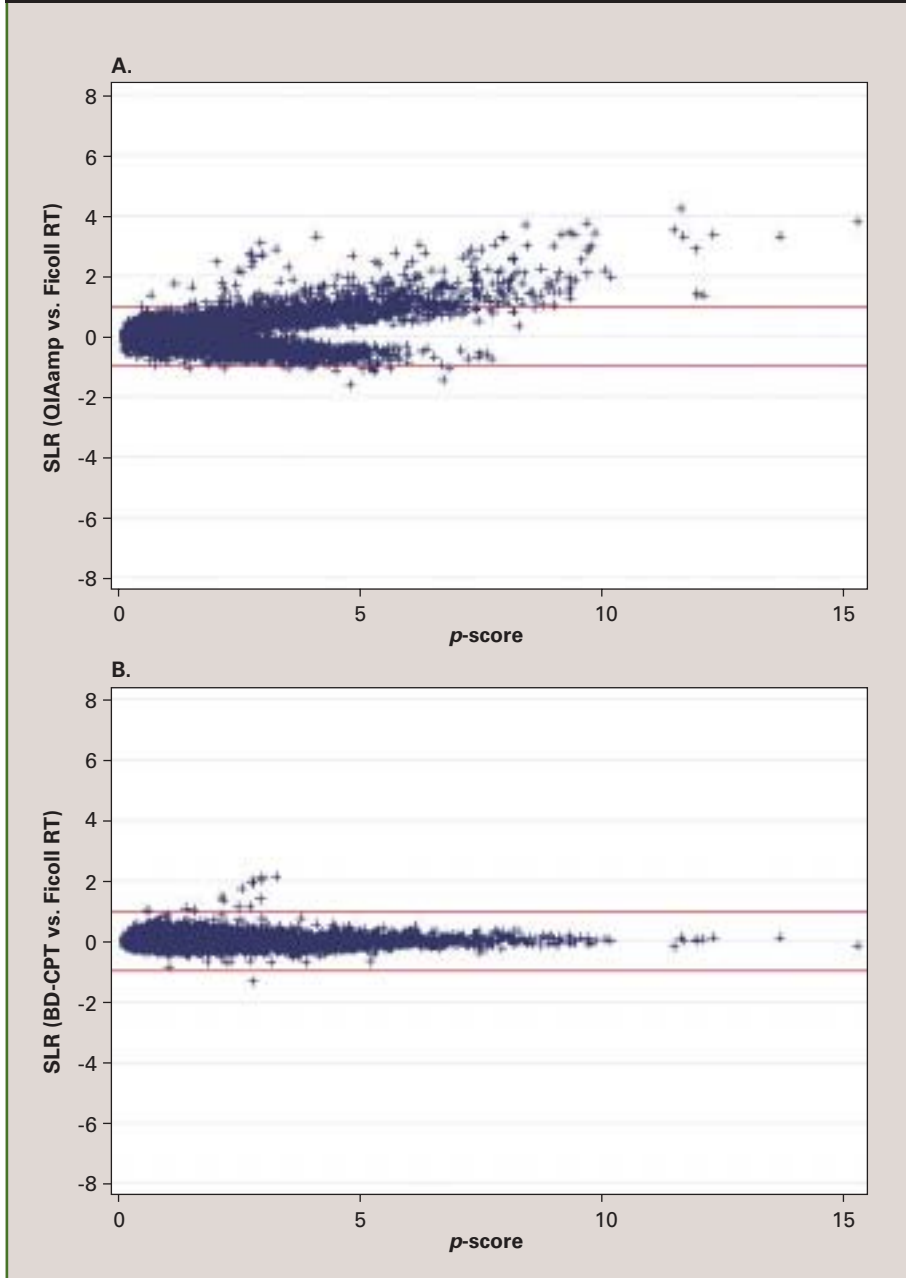
#### IMPACT ON EXPRESSION PROFILES - FICOLL CENTRIFUGATION VS BD-CPT VS. QIAAMP PROCESSING

To evaluate the differences between RNA isolation techniques, a direct comparison was performed among Ficoll centrifugation, BD-CPT tube, and QIAamp methods, using blood isolated from the same five individuals. Total RNA was isolated and labeled following the standard GeneChip Eukaryotic Labeling Assay and hybridized onto HG-U133A arrays. Analysis of Variation (ANOVA) was performed to identify the genes that were expressed differentially in the three methods. The results are plotted in Figure 10.

Unlike previous data analyzed using paired  $t$ -tests, this experiment compared data obtained from three different techniques at the same time. For each probe set, a single  $p$ -score was calculated from the three-way ANOVA analysis, and a higher  $p$ -score indicates a significant change in expression between at least two of the three samples. Figures 10A and 10B are both plotted against the same  $p$ -score.

As shown in Figure 10A, a large number of genes were altered between QIAamp and Ficoll methods (see Appendix 4 for the list of probe sets). 287 probe sets were expressed at a higher level in QIAamp samples, compared with 26 probe sets that were present at a higher level in Ficoll. This may be due to the fact that more cell types were isolated using QIAamp than with Ficoll. Similar results were also obtained comparing QIAamp and BD-CPT samples (not shown). In contrast, in Figure 10B, very few differences are observed between BD-CPT and Ficoll.

**Figure 10:** Comparison of Signal Log Ratios (SLR) from samples obtained from BD-CPT, Ficoll centrifugation, and QIAamp. **A.** The y-axis shows the SLR computed by MAS 5.0, comparing QIAamp to Ficoll (baseline for SLR calculation). On the y-axis, 0 represents no change, +1 and -1 represent genes that are expressed 2-fold higher or 2-fold lower, respectively, in QIAamp samples vs. Ficoll samples. The x-axis shows the  $p$ -score for ANOVA, derived by taking the negative log of the ANOVA  $p$ -value. **B.** The axes are as described above, except that the y-axis shows the SLR comparing BD-CPT to Ficoll (baseline for SLR calculation).



A set of signature genes was selected for red blood cells, granulocytes, and mononuclear cells, as described in Materials and Methods, and are listed in Appendix 1. Expression of these signature genes was analyzed. The results are shown in Figure 11.

Figures 11A and 11B show that the granulocyte markers (shown in blue) are more highly expressed in the QIAamp samples. This is consistent with the fact that QIAamp preparations retain this cellular fraction, whereas BD-CPT and Ficoll preparations exclude it. The mononuclear cell markers (shown in green) show greater expression in the BD-CPT and Ficoll samples, consistent with their selective enrichment by these procedures. Red blood cell markers, shown in red, also appear to be more highly expressed in the QIAamp samples, suggesting that the erythrocyte lysis procedure may not completely remove red blood cells.

Figure 11C shows that mononuclear cells are expressed similarly in both Ficoll and BD-CPT, but some red blood cell markers (shown in red) are expressed more in the BD-CPT samples. When cell fractions were collected, a reddish color in the cell pellets was observed in the BD-CPT purified fraction, indicating that some red blood cells were present. This observation is consistent with the molecular findings shown here. Researchers should be aware of this small amount of contamination of red blood cells in the mononuclear cell fraction.

Figures 10 and 11 reveal global changes in expression data among the different blood processing techniques used, as well as differences in cell type signatures. However, it was observed that there was little overlap between the signature genes

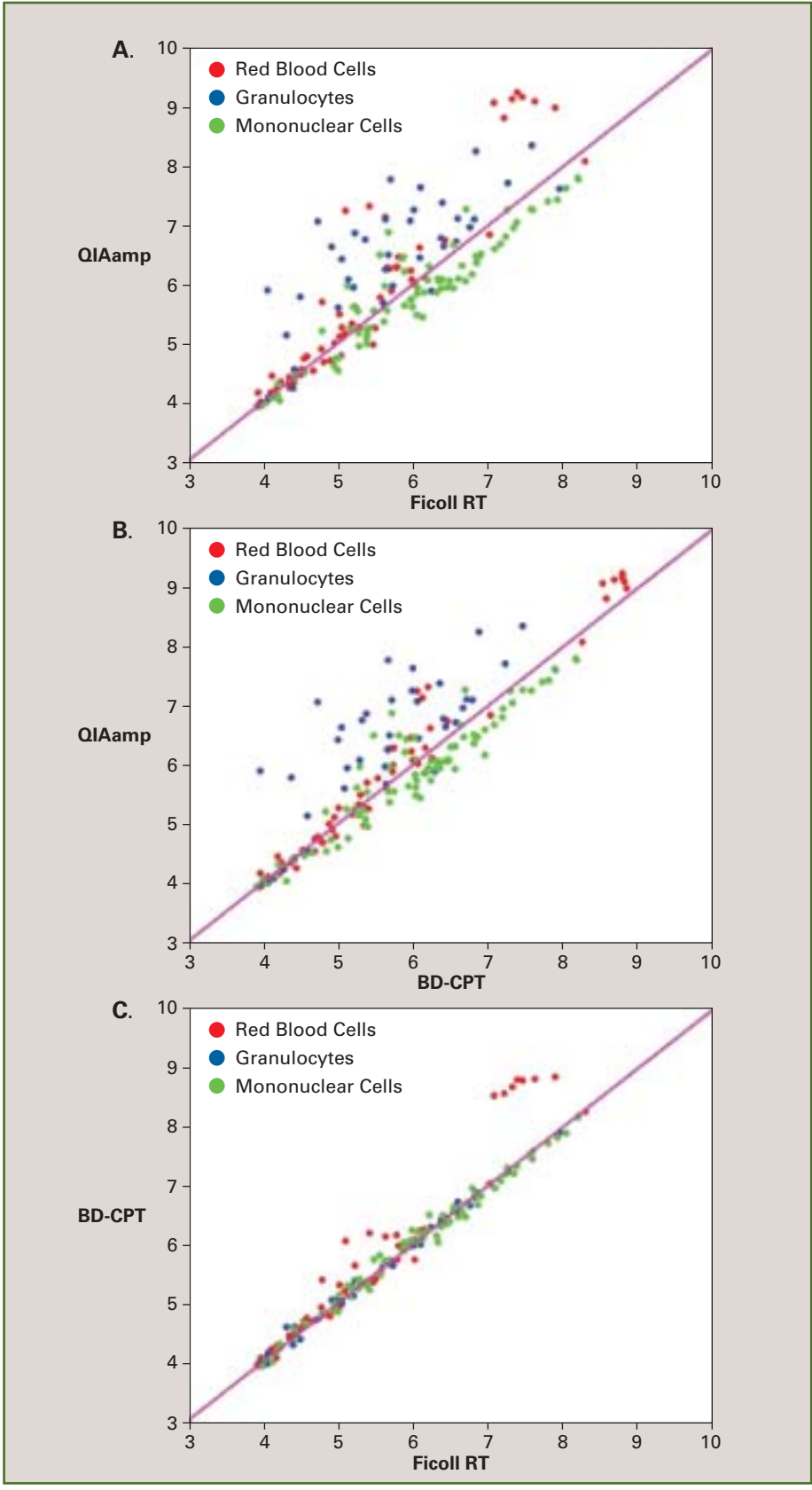


**Figure 11:** Scatter plots of signature genes in samples from different blood processing methods. Three groups of signature genes are shown, and color-coded as indicated. For comparison, the unity line is shown in magenta. Each data point represents the average expression level ( $n = 5$ ) after natural log transformation, computed as described in the Materials and Methods section. Comparison between two methods is plotted with the expression level of signature genes represented on the two axes in each graph:

**A.** The y-axis shows signature gene expression levels for QIAamp, and the x-axis for Ficoll.

**B.** The y-axis shows signature gene expression levels for QIAamp, and the x-axis for BD-CPT.

**C.** The y-axis shows signature gene expression levels for BD-CPT, and the x-axis for Ficoll.

and the genes considered to be most significantly changed. This could reflect the high stringency of the confidence threshold we used (Bonferroni correction).

**IMPACT ON EXPRESSION PROFILES - QIAAMP VS. PAXGENE**

To directly compare the two non-PBMC methods, QIAamp and PAXgene, isolation techniques, blood from five donors was prepared for GeneChip HG-U133A arrays by either a QIAamp or PAXgene protocol. As shown earlier, PAXgene RNA gave a reduced detection sensitivity on the arrays as determined by the Percent Present calls (Figure 5). A paired  $t$ -test was performed to identify genes that were expressed differently in each method. The results are plotted in Figure 12.

Figure 12 shows that 29 probe sets are significantly changed, of which 22 are present at higher levels in PAXgene and 7 in QIAamp. The differentially expressed genes are listed in Appendix 5.

**Figure 12:** Signal Log Ratios (SLR) of QIAamp and PAXgene samples. The y-axis shows the SLR computed by MAS 5.0, comparing results from QIAamp to PAXgene (baseline for SLR calculation). On the y-axis, 0 represents the no change line, the two horizontal lines +1 and -1 represent probesets that are expressed 2-fold higher or 2-fold lower respectively. The x-axis shows the  $p$ -score, defined here as the negative log of the  $p$ -value from the paired  $t$ -test. A higher  $p$ -score indicates higher statistical significance of change. The vertical line represents the Bonferroni 95% significance cutoff. Probesets to the right of the vertical line are significantly different between the two methods.

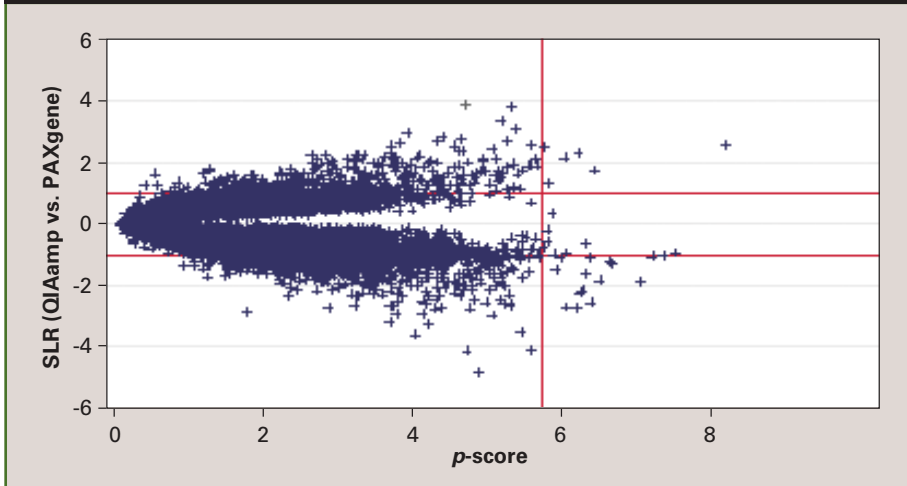


Figure 13 shows the expression of the three groups of signature genes in these two methods. The probe sets which are markers of red blood cells (shown in red) are more abundant in the PAXgene samples compared to QIAamp, confirming that the erythrocyte lysis procedure in QIAamp reduced the red blood cell population in the process. The expression levels for signature genes of granulocytes (shown in blue) and mononuclear cells (shown in green) appear comparable between the two methods, although there may have been a slight increase in expression of these markers in QIAamp samples.

#### IMPACT ON EXPRESSION PROFILES – PAXGENE VS. BD-CPT

To further define the differences associated with different blood RNA isolation techniques as described in Tables 1 and 2, the variability in results from either the PBMC fraction (BD-CPT) or whole blood (PAXgene) was quantified. In this study, samples were collected from four volunteers and divided for the two

processing methods (data set provided by GlaxoSmithKline, Stevenage, UK). Paired  $t$ -tests were performed to analyze the differences in the sensitivity and variability.

It was shown previously that reduced sensitivity using RNA isolated from whole blood was observed with respect to Percent Present calls (Figure 5). To evaluate the variability associated with each blood processing techniques, the coefficient of variation (CV%) was examined on a probe set-by-probe set basis to compare the two methods across the same four individuals. Figure 14 represents the CV% plotted against Signal.

As seen in Figure 14, there was greater variability within samples prepared using the PAXgene method than the BD-CPT method. The probe sets with higher variability in PAXgene samples were distributed relatively evenly across the entire range of intensities.

**Figure 13:** Scatter plot of the signature genes from samples prepared by QIAamp or PAXgene. Three groups of signature genes are shown, and color-coded as indicated. For comparison, the unity line is shown in magenta. Each data point represents the average expression level ( $n = 5$ ) after natural log transformation, computed as described in the Materials and Methods section. Comparison between two methods is plotted with the expression level of signature genes represented on the two axes. The y-axis shows signature gene expression levels for QIAamp, and the x-axis for PAXgene.

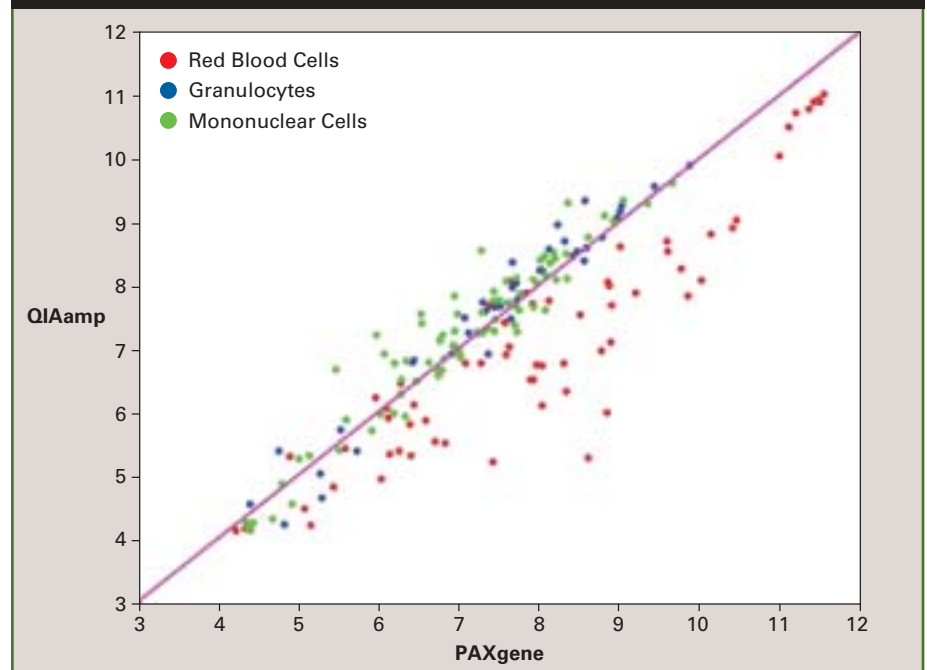
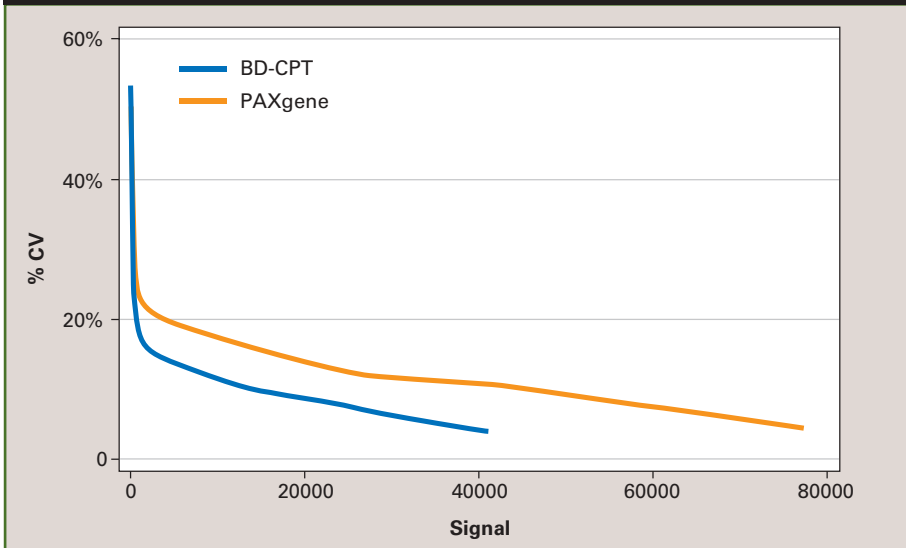


**Figure 14:** Comparison of variability of BD-CPT and PAXgene. The mean Signal value for each probe set within each method across all four individuals was computed, and the Standard Deviation derived. The CV% (Standard Deviation/Mean) was plotted against the Average Signal for that probe set.



A paired *t*-test was used to identify the genes that showed differential expression between these two methods. The results are shown in Figure 15.

A total of 208 probe sets were identified to have Signal values that were significantly different, with 84 and 124 probe sets displaying higher or lower intensity, respectively, in the PAXgene preparation. A complete list of these probe sets is included in Appendix 6 for reference.

The probe sets displaying higher expression in the PAXgene method may represent the genes expressed in the cell types that are excluded in the BD-CPT preparation. In contrast, the probe sets more highly represented in the BD-CPT method could include low expression genes that are not readily detected in the PAXgene protocol, as well as those genes that may be induced consistently by the *ex vivo* manipulation during BD-CPT manipulation.

To verify the expression analysis results obtained by the two methods, the expression pattern of signature genes was also analyzed. The results are shown in Figure 16.

The signature genes for cell types only represented in the PAXgene preparation, namely, red blood cells (shown in red), and granulocytes (shown in blue), display drastically lower expression levels in BD-CPT samples, but not in PAXgene samples. This was expected results, as BD-CPT samples contain only mononuclear cells while PAXgene samples are obtained from whole blood.

**Figure 15:** Comparison of Signal Log Ratios (SLR) from samples obtained from PAXgene and BD-CPT. The x-axis shows the SLR computed by MAS 5.0, comparing results from PAXgene vs. BD-CPT. On the y-axis, 0 represents the no change line, +1 and -1 represent genes that are expressed 2-fold more or 2-fold less. The x-axis shows the *p*-score, defined here as the negative log of the *p*-value from the paired *t*-test. The vertical line represents the Bonferroni 95% significance cutoff. Probe sets to the right of the vertical line are significantly different between the two methods.

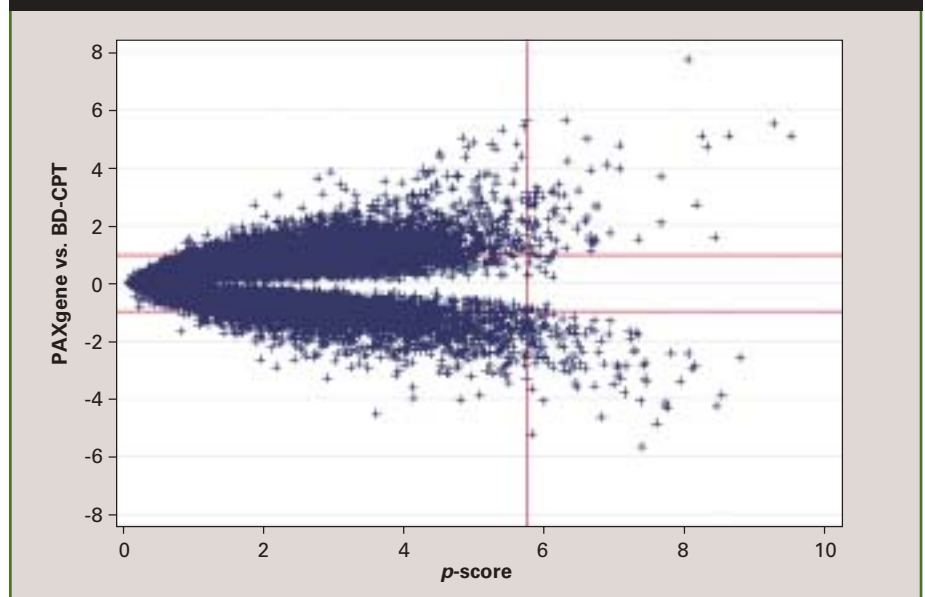
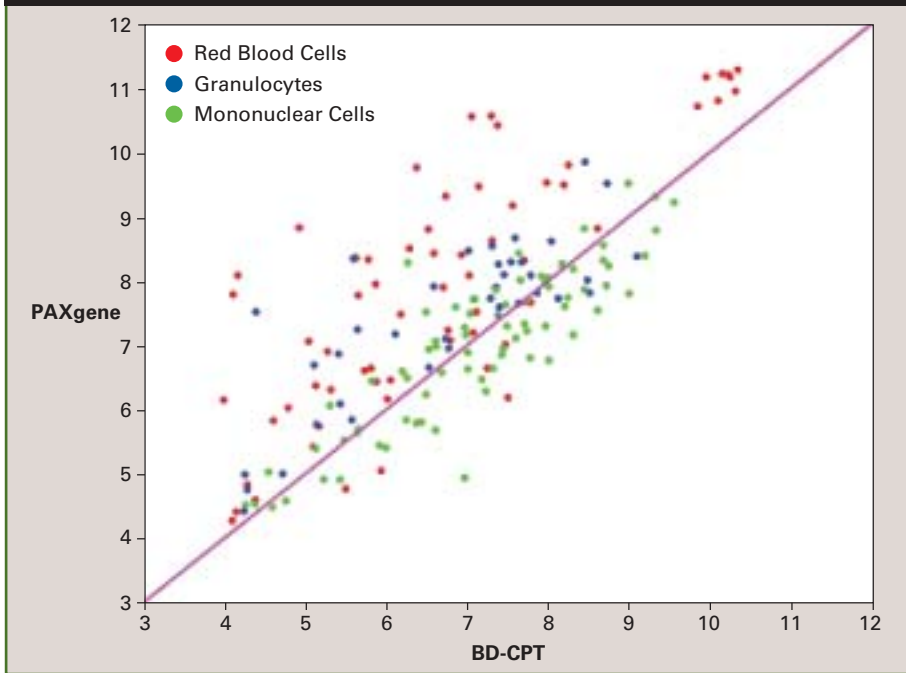


**Figure 16:** Scatter plot of the signature genes from samples prepared by PAXgene or BD-CPT. Three groups of signature genes are shown, and color-coded as indicated. For comparison, the unity line is shown in magenta. Each data point represents the average expression level (n = 5) after natural log transformation, computed as described in the Materials and Methods section. The y-axis shows signature gene expression levels for PAXgene, and the x-axis for BD-CPT.



## Main Findings

In conclusion, our analyses have revealed the following observations:

- Expression array results were similar for experiments conducted with the Ficoll gradient technique performed at room temperature and 8°C.
- Expression array results were comparable for experiments conducted with either BD-CPT or Ficoll centrifugation methods.
- Many changes in gene expression data were observed when blood was incubated overnight before Ficoll processing.
- QIAamp, Ficoll, and BD-CPT methods generated comparable detection sensitivity for identical samples, whereas the PAXgene method resulted in drastic differences in expression data and detection sensitivity.

## Discussion

This Technical Note reports GeneChip array data obtained on RNA samples prepared from various blood processing methods, such as the PAXgene, QIAamp, Ficoll, and BD-CPT techniques. Results presented here focus on the impact each method has on expression profiles. This information should provide insight for scientists to help them make an informed decision on which method is most suitable to use for their own research when they are considering various blood protocols in conjunction with GeneChip expression microarrays.

### RECOMMENDATIONS

Because each method varies from the others, it is recommended that one single method be used consistently throughout a study in order to obtain meaningful results. Due to the fact that research parameters and experimental conditions

may limit the blood isolation protocol choice, scientists should take these variables into account before initiating large studies in order to be able to use the same blood isolation technique consistently throughout.

In addition to the main findings listed above, several recommendations to consider are summarized here:

### *Storage of Blood Before Processing*

Results suggest that storing blood for a prolonged period of time prior to processing negatively affects the results. In this study, an overnight storage scenario before Ficoll preparation was compared to Ficoll preparation conducted immediately after blood was drawn. It was found that the delay in blood processing resulted in significant changes in expression profiles compared with the samples prepared immediately. Therefore, it would be beneficial to reduce the time of storage and transport to minimize the effect, and consequently, improve the quality of experimental results. Ideally, RNA should be isolated immediately after blood samples are drawn, and the frozen RNA samples can then be transported and stored. A time-course study is necessary to assess whether there is a shorter period of time for storage or transport of blood that may not be detrimental to the results.

### *Points to consider for selecting blood processing methods*

It is recommended that users carefully evaluate their research requirements, as well as constraints, and use the data presented here to help choose the method that best matches their needs. Some of the basic considerations in selecting a method include:

- Cell types of interest: This may limit the method of choice. For example, if neutrophils are the primary cells being studied, PAXgene and QIAamp are the only options of those discussed in this Technical Note, whereas the PBMC fraction isolated by the BD-CPT or Ficoll methods may not be appropriate.

- Availability of equipment and trained personnel at the site of blood draw: This can be critical since the different methods require varying degrees of blood manipulation following blood draw, ranging from zero processing, in the case of PAXgene, to relatively complex, skilled processing, such as preparation and running the Ficoll gradient.
- Assay sensitivity requirements: Different methods displayed varying levels of sensitivity with the GeneChip microarrays. Depending on research requirements, this factor may be critical. Using a method with relatively compromised sensitivity, such as PAXgene, may be acceptable for some applications. For others it may be beneficial to perform additional fractionation, to isolate only the cells belonging to a subtype.
- Tolerance to increased assay variability: Although not included in this study, it has been speculated that increasing the number of replicates may help reduce variability in general. Therefore, if constrained by other requirements, adequate planning and design of experiments may allow for tolerance of the increased variability observed in some of these methods.

Additional information is provided in this Technical Note, such as the list of signature genes, as well as those that were documented in our study to be significantly different using various methods. Although detailed analyses have not been performed on the expression pattern of all of the genes listed, this information may be used as a reference by users for comparison purposes in the initial assessment of the quality of their data.

## Contributors

This study was performed at the Molecular Tumor Biology and Tumor Immunology Unit, University of Cologne, Germany, by Dr. Svenja Debey, Ulrike Diening, and Prof. Joachim L. Schultze, in collaboration with Affymetrix Genomics Collaborations (Dr. Raji Pillai), Data AnalysisTeam (Dr. David Finkelstein and Dr. John Martin), and Affymetrix Product Marketing (Dr. Yan Zhang-Klompus).

The data from the PAXgene – BD-CPT study was contributed by Dr. Chris Clayton and Simon Graham, Transcriptome Analysis Department, GlaxoSmithKline, Stevenage, U.K., as was a list of cell type-specific genes. We thank Dr. Gavin Sherlock of the Stanford Microarray Center and Dr. Alan Williams of the Affymetrix Bioinformatics Department for assistance with mapping the IMAGE clones from Whitney *et al* to the HG-U133 arrays, and Dr. Michael Morrissey of Millennium Pharmaceuticals, Cambridge, Massachusetts, U.S.A. for the list of probe sets considered to be monocyte-specific.

## REFERENCE

- DePrimo, S.E. *et al. BMC Cancer* **3**: 1-12 (2003).
- Fauci, Braunwalder, Isselbacher, Wilson, Martin, Kasper, Hauser, Longo. *Harrison's Principles of Internal Medicine – international edition* (14th edition). Vol. I Appendix A-5. *McGraw-Hill*, New York, St.Louis, San Francisco (1998).
- Tukey, J.E. *Exploratory Data analysis*. Cambridge, MA. *Addison-Wesley* (1997).
- Whitney, A.R. *et al. Proc. Natl. Acad. Sci. USA* **100**: 1896-1901 (2003).

## Material and Methods

### BLOOD CELL FRACTIONATION AND TOTAL RNA ISOLATION TECHNIQUES

Blood was collected from healthy individuals after informed consent following the institutional review board at the University of Cologne.

- Ficoll-Hypaque – Citrate blood collection tubes were used to collect 50 mL of peripheral venous blood from each healthy volunteer. The blood samples were then transported within 15 minutes to the laboratory and either stored for the lengths of time indicated in the Results section, or processed immediately. Ficoll-Hypaque density centrifugation was performed following standard methodology. The samples were divided into two 25 mL aliquots and centrifuged at 400 x g for 7 minutes at either 18 to 20°C (room temperature, RT) or 8°C. The upper plasma phase was removed and the rest of the sample was diluted with an equal volume of 1X PBS and mixed by pipetting. The Ficoll gradient centrifugation was then performed either at room temperature or at 8°C. For the 8°C samples, the centrifuge, PBS, and Ficoll were cooled down 30 minutes prior to use. The diluted blood samples were overlaid on 12.5 mL of Ficoll and centrifuged at 800 x g for 25 minutes without brake. The interphase was then transferred to 30 mL of 1X PBS and mixed by inverting the tubes, and centrifuged at 500 x g for 10 minutes with brake. The supernatant was discarded and the cell pellet was resuspended in 20 mL of 1X PBS by pipetting. As determined by trypan blue staining, for all experiments, over 95% of the cells obtained were viable. The cells were pelleted by centrifugation at 500 x g for 5 minutes with brake and the supernatant was removed completely.

One mL of the TRIzol® Reagents (Invitrogen, CA, USA) was added to every  $1 \times 10^7$  cells and the cells were lysed by repetitive pipetting and incubated for 5 minutes at ambient temperature to permit complete dissociation of nucleoprotein complexes. The samples were stored at  $-80^\circ\text{C}$  until total RNA isolation (for details, see the RNA Isolation section below).

- **BD-CPT – BD Vacutainer™ CPT™ Sodium Citrate Tubes** (Becton Dickinson, NJ, USA) were used to collect peripheral venous blood from healthy volunteers. Three tubes were collected from each individual with 8 mL of blood in each tube. The blood samples were mixed by gently inverting the tubes 5 times, prior to transport to the laboratory for processing. The transition was kept as short as possible (up to 15 minutes) and the tubes were kept upright at ambient temperature. Immediately before centrifugation, the blood samples were remixed by inverting the tubes 8 to 10 times. Centrifugation was performed at  $1,650 \times g$  for 20 minutes in a swinging bucket centrifuge at room temperature ( $18^\circ\text{C}$ ) with brake. The upper layer was transferred to a new tube containing 30 mL of 1X PBS. Cells were centrifuged at  $500 \times g$  for 10 minutes with brake and supernatant was discarded. The cell pellet was resuspended in 20 mL of 1X PBS. As indicated by Trypan Blue exclusion test, cell viability was always  $>95\%$ . The cells were centrifuged again at  $500 \times g$  for 5 minutes with brake and the supernatant was removed. One mL of the TRIzol® Reagents (Invitrogen, CA, USA) was added to every  $1 \times 10^7$  cells and the cells were lysed by repetitive pipetting and incubated for 5 minutes at ambient temperature to permit complete dissociation of nucleoprotein complexes. The samples were stored at  $-80^\circ\text{C}$  until total RNA isolation (for details, see the RNA Isolation section below).

- **RNA Isolation –** After thawing, 0.2 mL of chloroform per mL of the TRIzol® Reagents was added to each sample. The tubes were shaken by hand for 15 seconds and incubated for 3 minutes at room temperature. The samples were then centrifuged at 13,000 rpm in a microcentrifuge for 10 minutes at  $4^\circ\text{C}$ . Following centrifugation, the upper aqueous phase was transferred to a fresh tube and the RNA was precipitated by the addition of 0.5 mL of isopropanol per mL of the TRIzol Reagent used in the initial homogenization. The samples were incubated for 10 minutes at room temperature and then centrifuged at 13,000 rpm in a microcentrifuge for 30 minutes at  $4^\circ\text{C}$ . The supernatant was removed and the RNA pellets were washed twice by adding 1 mL of 80% ethanol, mixed by vortexing and centrifuged at 13,000 rpm for 5 minutes at  $4^\circ\text{C}$ . After washing, the RNA pellets were air-dried for 5-10 minutes, dissolved in RNAase-free water and incubated for 5 to 10 minutes at  $55^\circ\text{C}$ . The RNA was purified with the RNeasy MinElute Cleanup Kit (QIAGEN GmbH, Germany).
- **PAXgene™ Blood RNA Isolation System –** Three PAXgene Blood RNA Tubes (QIAGEN GmbH, Germany) with 2.5 mL blood in each tube were used to collect peripheral venous blood from each healthy volunteer following the manufacturer's recommended procedure, including the optional DNase digestion step. The RNA from the three tubes for each individual was pooled prior to quantitation. The RNA was then concentrated with the RNeasy MinElute Cleanup Kit (QIAGEN GmbH, Germany).
- **QIAamp® RNA Blood Mini Kits –** Citrate blood collection tubes were used to collect peripheral venous blood from healthy volunteers. 9 to 18 mL of blood samples were divided into 1.5 mL aliquots or less. No more than  $1 \times 10^7$  cells were loaded on one column. The

samples were processed individually with the QIAamp RNA Blood Mini Kits (QIAGEN GmbH, Germany) following the manufacturer's recommended procedure including the optional DNase digestion step. RNA was pooled prior to quantitation. The RNA was then concentrated with the RNeasy MinElute Cleanup Kit (QIAGEN GmbH, Germany).

#### FLOW CYTOMETRY

Cell phenotype was defined by four-color staining performed on PBMCs using the following antibodies: FITC conjugated anti-CD3, -CD71, -CD45RA (Pharmingen), PE-conjugated anti-CD4 (Pharmingen), PerCP-conjugated anti-CD19, -CD20, -CD8 (Becton Dickinson), APC-conjugated anti-CD14, -CD69, -CD25, -CD45RO (Pharmingen), Simultest anti-CD3/16+56 (Becton-Dickinson), and corresponding mouse IgG controls: Simultest  $\gamma 1 \gamma 2a$ , APC-conjugated anti- $\gamma 2a$  (Becton Dickinson), PerCP-conjugated  $\gamma 1$  (Pharmingen).

In brief, cells were washed with 2 mL cell wash (Becton Dickinson) and centrifuged for 5 minutes at  $450 \times g$  with brake. Supernatant was removed and the cells were resuspended in 100  $\mu\text{L}$  cell wash and stained for 20 minutes at  $4^\circ\text{C}$  with the appropriate antibodies. After washing, cells were fixed with cell wash containing 2% (v/v) formaldehyde. Samples were run on a FACS Calibur (Becton Dickinson) and analyzed with CellQuest 3.3 software.

#### GENECHIP® TARGET LABELING AND ARRAY HYBRIDIZATION

Total RNA (5-20  $\mu\text{g}$ ) obtained from each sample was labeled following the standard target labeling protocol as described in the GeneChip® Expression Analysis Technical Manual. The amount of cRNA obtained from the *in vitro* transcription reaction was quantified using a spectrophotometer. Following fragmentation, 10  $\mu\text{g}$  of cRNA target were hybridized to HG-U133A arrays.

#### GENECHIP ARRAY DATA STATISTICAL ANALYSIS

The array Signal values from MAS 5.0 were normalized to a target intensity of 100 (in most cases, scaling factor (s.f.) was  $< 3$ ). In some of the PAXgene or QIAamp samples, the s.f. exceeded this value (5-6)). Then, the value 50 (roughly twice the Standard Deviation of the Background) was added to all measurements. This serves to stabilize the variance of Signal and Background near the low end of expression, and has very little effect on the high end of data (Affymetrix Inc, unpublished observations). After transformation, the data more closely conform to the assumptions that underlie *t*-test and ANOVA analyses. Alternatives to variance stabilizing approaches may also be used, such as filtering based on Detection Calls.

Following this procedure, data were subjected to a natural log transformation so that each data point has more equivalent influence on the final outcome.

When results from two RNA isolation methods were compared where the blood samples were obtained from the same five individuals, a two-sample *t*-test with equal variances was used.

When results from three methods were compared with blood from the same five individuals, ANOVA analysis was performed.

All these analytical methods identified genes that were changed among the different blood preparation methods. These genes vary in terms of magnitude of change, as well as statistical significance of change. Either criterion may be used as a filter to select genes for further analyses. Genes selected by magnitude of change may include those that do not show consistent change. Conversely, genes selected based on stringent statistical cut-off may include some genes that show very subtle changes.

We selected a statistical approach, namely the Bonferroni correction, as a threshold.

This stringent approach selects only genes that can be considered true positives, with no false positives present (95% confidence). The disadvantage of this approach is that in requiring no false positives, we fail to select some authentic changes, i.e., we generate some false negatives. Less stringent thresholds may be used, for example, those based on the False Discovery Rate (FDR, Yoav Benjamini, Tel Aviv University).

These analyses were performed using the STATA/S.E. 8.0 software package (College Station, Texas, U.S.A) and the MATLAB 6.5 software package (The MathWorks, Natick, Massachusetts, U.S.A).

#### GENERATION OF SIGNATURE GENES FOR DIFFERENT BLOOD CELL TYPES

HG-U133A probe sets that were specific to different cell types in blood based on information were identified from several sources listed below:

- 29 genes were found to be expressed in monocytes but demonstrated very little or no expression in other blood cells (Millennium Pharmaceuticals, Cambridge, MA, U.S.A).
- 12 genes were used as markers of different blood cells (GlaxoSmithKline, Stevenage, U.K.). These were originally identified in the GeneChip® Human Genome U95Av2 set of arrays, but were mapped to HG-U133A using the NetAffx™ Analysis Center ([www.affymetrix.com](http://www.affymetrix.com)).
- A recent publication by Whitney *et al*, (2003) showed seven groups of genes, some classified according to cell type, others according to variability seen among the individuals studied. 797 original IMAGE clone IDs were represented in these seven groups. We identified 604 probe sets on the GeneChip HG-U133 Array Set corresponding to 555 of the

797 IMAGE clones based on IMAGE clone identifiers and GenBank sequence identifiers. These were included in the selection of the signature genes.

- A set of 14 probe sets that represented different forms of hemoglobin on the HG-U133A array were added to the signature list.

The signature genes were compiled from the above sources and a final list was generated based on our ability to map them with confidence to the HG-U133 array set. This list contains 181 probe sets. Of these, 78 probe sets are for mononuclear cells (monocytes and lymphocytes), 38 for granulocytes (neutrophils and eosinophils), and 65 for red blood cells (erythrocytes and reticulocytes). It is important to note that for many of these probe sets (particularly those derived from Whitney *et al*), their expression primarily in the respective cell types has not been confirmed experimentally on GeneChip arrays. They were used here solely for the purpose of cross-validation and verification of analysis, and should be used as reference only. A complete listing of these signature gene IDs on HG-U133A arrays is provided in Appendix 1.

## Appendix 1: Signature genes for different blood cell types.

Blood Fraction	Cell Type	Source	Probe Set ID	Description	Symbol	Blood Fraction	Cell Type	Source	Probe Set ID	Description	Symbol
Mono-nuclear cells	Lymphocytes	GSK	203547_at	CD4 antigen (p55)	CD4			Whitney <i>et al.</i>	209813_x_at	T cell receptor gamma locus	TRG
		Whitney <i>et al.</i>	203104_at	colony stimulating factor 1 receptor, formerly McDonough feline sarcoma viral (v-fms) oncogene homolog	CSF1R		Whitney <i>et al.</i>	209995_s_at	T-cell leukemia/lymphoma 1A	TCL1A	
		Whitney <i>et al.</i>	203290_at	major histocompatibility complex, class II, DQ alpha 1	HLA-DQA1		Whitney <i>et al.</i>	210164_at	granzyme B (granzyme 2, cytotoxic T-lymphocyte-associated serine esterase 1)	GZMB	
		Whitney <i>et al.</i>	203413_at	NEL-like 2 (chicken)	NELL2		Whitney <i>et al.</i>	210321_at	similar to granzyme B (granzyme 2, cytotoxic T-lymphocyte-associated serine esterase 1) (H. sapiens)	CTLA1	
		Whitney <i>et al.</i>	203828_s_at	natural killer cell transcript 4	NK4		Whitney <i>et al.</i>	212827_at	immunoglobulin heavy constant mu	IGHM	
		Whitney <i>et al.</i>	203932_at	major histocompatibility complex, class II, DM beta	HLA-DMB		Whitney <i>et al.</i>	212998_x_at	major histocompatibility complex, class II, DQ beta 1	HLA-DOB1	
		Whitney <i>et al.</i>	204655_at	chemokine (C-C motif) ligand 5	CCL5		Whitney <i>et al.</i>	212999_x_at	major histocompatibility complex, class II, DQ beta 1	HLA-DOB	
		Whitney <i>et al.</i>	204661_at	CDW52 antigen (CAMPATH-1 antigen)	CDW52		Whitney <i>et al.</i>	213193_x_at	T cell receptor beta locus	TRB	
		Whitney <i>et al.</i>	205049_s_at	CD79A antigen (immunoglobulin-associated alpha)	CD79A		Whitney <i>et al.</i>	213425_at	Homo sapiens cDNA FLJ11441 fis, clone HEMBA1001323, mRNA sequence		
		Whitney <i>et al.</i>	205291_at	interleukin 2 receptor, beta	IL2RB		Whitney <i>et al.</i>	213958_at	CD6 antigen	CD6	
		Whitney <i>et al.</i>	205484_at	SHP2 interacting transmembrane adaptor	SIT		Whitney <i>et al.</i>	214450_at	cathepsin W (lymphopain)	CTSW	
		Whitney <i>et al.</i>	205488_at	granzyme A (granzyme 1, cytotoxic T-lymphocyte-associated serine esterase 3)	GZMA		Whitney <i>et al.</i>	214470_at	killer cell lectin-like receptor subfamily B, member 1	KLRB1	
		Whitney <i>et al.</i>	205495_s_at	granulysin	GNLY		Whitney <i>et al.</i>	214617_at	Perforin, mRNA sequence		
		Whitney <i>et al.</i>	205758_at	CD8 antigen, alpha polypeptide (p32)	CD8A		Whitney <i>et al.</i>	218805_at	immune associated nucleotide 4 like 1 (mouse)	IAN4L1	
		Whitney <i>et al.</i>	205798_at	interleukin 7 receptor	IL7R		Whitney <i>et al.</i>	221491_x_at	major histocompatibility complex, class II, DR beta 5	HLA-DRB5	
		Whitney <i>et al.</i>	205826_at	myomesin (M-protein) 2, 165kDa	MYOM2		Whitney <i>et al.</i>	221601_s_at	regulator of Fas-induced apoptosis	TOSO	
		Whitney <i>et al.</i>	205831_at	CD2 antigen (p50), sheep red blood cell receptor	CD2		Whitney <i>et al.</i>	221602_s_at	regulator of Fas-induced apoptosis	TOSO	
		Whitney <i>et al.</i>	205861_at	Spi-B transcription factor (Spi-1/PU.1 related)	SPIB		Whitney <i>et al.</i>	221736_at	Homo sapiens cDNA: FLJ23118 fis, clone LNG07969, mRNA sequence		
		Whitney <i>et al.</i>	206150_at	tumor necrosis factor receptor superfamily, member 7	TNFRSF7		Whitney <i>et al.</i>	221738_at	KIAA1219 protein	KIAA1219	
		Whitney <i>et al.</i>	206337_at	chemokine (C-C motif) receptor 7	CCR7		Whitney <i>et al.</i>	221756_at	hypothetical protein MGC17330	MGC17330	
		Whitney <i>et al.</i>	206666_at	granzyme K (serine protease, granzyme 3; tryptase II)	GZMK		Whitney <i>et al.</i>	221757_at	hypothetical protein MGC17330	MGC17330	
		Whitney <i>et al.</i>	208894_at	major histocompatibility complex, class II, DR alpha	HLA-DRA						
		Whitney <i>et al.</i>	209172_s_at	centromere protein F, 350/400ka (mitosin)	CENPF		Monocytes	GSK	201743_at	CD14 antigen	CD14
		Whitney <i>et al.</i>	209312_x_at	major histocompatibility complex, class II, DR beta 1	HLA-DRB1		Millennium	201118_at	phosphogluconate dehydrogenase	PGD	
		Whitney <i>et al.</i>	209480_at	major histocompatibility complex, class II, DQ beta 1	HLA-DQB1		Millennium	202086_at	myxovirus (influenza virus) resistance 1, interferon-inducible protein p78 (mouse)	MX1	
		Whitney <i>et al.</i>	209508_x_at	CASP8 and FADD-like apoptosis regulator	CFLAR		Millennium	202687_s_at	tumor necrosis factor (ligand) superfamily, member 10	TNFSF10	
		Whitney <i>et al.</i>	209670_at	T cell receptor alpha locus	TRA		Millennium	202688_at	tumor necrosis factor (ligand) superfamily, member 10	TNFSF10	
		Whitney <i>et al.</i>	209671_x_at	T cell receptor alpha locus	TRA		Millennium	202877_s_at	complement component 1, q subcomponent, receptor 1	C1QR1	
		Whitney <i>et al.</i>	209728_at	major histocompatibility complex, class II, DR beta 4	HLA-DRB4		Millennium	203153_at	interferon-induced protein with tetratricopeptide repeats 1	IFIT1	

Blood Fraction	Cell Type	Source	Probe Set ID	Description	Symbol	Blood Fraction	Cell Type	Source	Probe Set ID	Description	Symbol
		Millennium	205789_at	CD1D antigen, d polypeptide	CD1D			Whitney <i>et al.</i>	203765_at	grancalcin, EF-hand calcium binding protein	GCA
		Millennium	205819_at	macrophage receptor with collagenous structure	MARCO			Whitney <i>et al.</i>	203805_s_at	hypothetical protein MGC45417	MGC45417
		Millennium	205844_at	vanin 1	VNN1			Whitney <i>et al.</i>	203806_s_at	Fanconi anemia, complementation group A	FANCA
		Millennium	206214_at	phospholipase A2, group VII (platelet-activating factor acetylhydrolase, plasma)	PLA2G7			Whitney <i>et al.</i>	203879_at	phosphoinositide-3-kinase, catalytic, delta polypeptide	PIK3CD
		Millennium	206978_at	chemokine (C-C motif) receptor 2	CCR2			Whitney <i>et al.</i>	204057_at	interferon consensus sequence binding protein 1	ICSBP1
		Millennium	207794_at	chemokine (C-C motif) receptor 2	CCR2			Whitney <i>et al.</i>	204118_at	CD48 antigen (B-cell membrane protein)	CD48
		Millennium	208130_s_at	thromboxane A synthase 1 (platelet, cytochrome P450, subfamily V)	TBXAS1			Whitney <i>et al.</i>	204309_at	cytochrome P450, subfamily XIA (cholesterol side chain cleavage)	CYP11A
		Millennium	208450_at	lectin, galactoside-binding, soluble, 2 (galectin 2)	LGALS2			Whitney <i>et al.</i>	204959_at	myeloid cell nuclear differentiation antigen	MNDA
		Millennium	209525_at	transmembrane 6 superfamily member 1	TM6SF1			Whitney <i>et al.</i>	205118_at	formyl peptide receptor 1	FPR1
		Millennium	210756_s_at	NOTCH 2 [Homo sapiens], mRNA sequence				Whitney <i>et al.</i>	205119_s_at	formyl peptide receptor 1	FPR1
		Millennium	212188_at	hypothetical protein BC013764	LOC115207			Whitney <i>et al.</i>	205159_at	colony stimulating factor 2 receptor, beta, low-affinity (granulocyte-macrophage)	CSF2RB
		Millennium	213566_at	ribonuclease, RNase A family, k6	RNASE6			Whitney <i>et al.</i>	205179_s_at	a disintegrin and metalloproteinase domain 8	ADAM8
		Millennium	214058_at					Whitney <i>et al.</i>	205180_s_at	a disintegrin and metalloproteinase domain 8	ADAM8
		Millennium	214329_x_at	tumor necrosis factor (ligand) superfamily, member 10	TNFSF10			Whitney <i>et al.</i>	205220_at	putative chemokine receptor; GTP-binding protein	HM74
		Millennium	215646_s_at	chondroitin sulfate proteoglycan 2 (versican)	CSPG2			Whitney <i>et al.</i>	205785_at	integrin, alpha M (complement component receptor 3, alpha; also known as CD11b (p170), macrophage antigen alpha polypeptide)	ITGAM
		Millennium	218231_at	N-acetylglucosamine kinase	NAGK			Whitney <i>et al.</i>	205786_s_at	integrin, alpha M (complement component receptor 3, alpha; also known as CD11b (p170), macrophage antigen alpha polypeptide)	ITGAM
		Millennium	218876_at	brain specific protein	CGI-38						
		Millennium	219093_at	hypothetical protein FLJ20701	FLJ20701						
		Millennium	219519_s_at	sialoadhesin	SN						
		Millennium	220005_at	G protein-coupled receptor 86	GPR86						
		Millennium	221060_s_at	toll-like receptor 4	TLR4						
Granulo-cytes	Neutrophils	GSK	207677_s_at	neutrophil cytosolic factor 4, 40kDa	NCF4						
		Whitney <i>et al.</i>	202269_x_at	guanylate binding protein 1, interferon-inducible, 67kDa	GBP1			Whitney <i>et al.</i>	205863_at	S100 calcium binding protein A12 (calgranulin C)	S100A12
		Whitney <i>et al.</i>	202270_at	guanylate binding protein 1, interferon-inducible, 67kDa	GBP1			Whitney <i>et al.</i>	205922_at	vanin 2	VNN2
		Whitney <i>et al.</i>	202625_at	v-yes-1Yamaguchi sarcoma viral related oncogene homolog	LYN			Whitney <i>et al.</i>	205945_at	interleukin 6 receptor	IL6R
		Whitney <i>et al.</i>	202626_s_at	v-yes-1Yamaguchi sarcoma viral related oncogene homolog	LYN			Whitney <i>et al.</i>	207857_at	leukocyte immunoglobulin-like receptor, subfamily A (with TM domain), member 2	LILRA2
		Whitney <i>et al.</i>	202748_at	guanylate binding protein 2, interferon-inducible	GBP2			Whitney <i>et al.</i>	209008_x_at	keratin 8	KRT8
		Whitney <i>et al.</i>	203140_at	B-cell CLL/lymphoma 6 (zinc finger protein 51)	BCL6			Whitney <i>et al.</i>	209606_at	pleckstrin homology, Sec7 and coiled/coiled domains, binding protein	PSCDBP
		Whitney <i>et al.</i>	203591_s_at	colony stimulating factor 3 receptor (granulocyte)	CSF3R			Whitney <i>et al.</i>	210225_x_at	leukocyte immunoglobulin-like receptor, subfamily B (with TM and ITIM domains), member 3	LILRB3
		Whitney <i>et al.</i>	203691_at	protease inhibitor 3, skin-derived (SKALP)	PI3			Whitney <i>et al.</i>	210660_at	leukocyte immunoglobulin-like receptor, subfamily A (with TM domain), member 1	LILRA1
		Whitney <i>et al.</i>	203760_s_at	Src-like-adaptor	SLA						
		Whitney <i>et al.</i>	203761_at	Src-like-adaptor	SLA						

Blood fraction	Cell type	Source	Probe Set ID	Description	Symbol	Blood fraction	Cell type	Source	Probe Set ID	Description	Symbol
		Whitney <i>et al.</i>	210772_at	formyl peptide receptor-like 1	FPRL1			Whitney <i>et al.</i>	211994_at	Homo sapiens, clone IMAGE:5264735, mRNA, mRNA sequence	
		Whitney <i>et al.</i>	210773_s_at	formyl peptide receptor-like 1	FPRL1			Whitney <i>et al.</i>	212312_at	BCL2-like 1	BCL2L1
		Whitney <i>et al.</i>	220000_at	sialic acid binding Ig-like lectin 5	SIGLEC5			Whitney <i>et al.</i>	212430_at	RNA-binding region (RNP1, RRM) containing 1	RNPC1
Red Blood Cells	Red Blood Cells	Whitney <i>et al.</i>	200633_at	ubiquitin B	UBB			Whitney <i>et al.</i>	212829_at	Homo sapiens cDNA FLJ13267 fis, clone OVARC1000964, mRNA sequence	
		Whitney <i>et al.</i>	200665_s_at	secreted protein, acidic, cysteine-rich (osteonectin)	SPARC			Whitney <i>et al.</i>	212867_at	ESTs, Weakly similar to A56429 I-kappa-B-related protein - human [H.sapiens]	
		Whitney <i>et al.</i>	201285_at	makorin, ring finger protein, 1	MKRN1			Whitney <i>et al.</i>	213060_s_at	chitinase 3-like 2	CHI3L2
		Whitney <i>et al.</i>	201912_s_at	G1 to S phase transition 1	GSPT1			Whitney <i>et al.</i>	213161_at	PP4189	LOC158427
		Whitney <i>et al.</i>	202129_s_at	sudD suppressor of bimD6 homolog (A. nidulans)	SUDD			Whitney <i>et al.</i>	213319_s_at	cold shock domain protein A	CSDA
		Whitney <i>et al.</i>	202130_at	sudD suppressor of bimD6 homolog (A. nidulans)	SUDD			Whitney <i>et al.</i>	214433_s_at	selenium binding protein 1	SELENBP1
		Whitney <i>et al.</i>	202131_s_at	sudD suppressor of bimD6 homolog (A. nidulans)	SUDD			Whitney <i>et al.</i>	215498_s_at	mitogen-activated protein kinase kinase 3	MAP2K3
		Whitney <i>et al.</i>	202364_at	MAX interacting protein 1	MXI1			Whitney <i>et al.</i>	215499_at	mitogen-activated protein kinase kinase 3	MAP2K3
		Whitney <i>et al.</i>	202387_at	BCL2-associated athanogene	BAG1			Whitney <i>et al.</i>	217748_at	CGI-45 protein	CGI-45
		Whitney <i>et al.</i>	202555_s_at	myosin, light polypeptide kinase	MYLK			Whitney <i>et al.</i>	218116_at	hepatocellular carcinoma-associated antigen 59	LOC51759
		Whitney <i>et al.</i>	203502_at	2,3-bisphosphoglycerate mutase	BPGM			Whitney <i>et al.</i>	221478_at	BCL2/adenovirus E1B 19kDa interacting protein 3-like	BNIP3L
		Whitney <i>et al.</i>	203966_s_at	protein phosphatase 1A (formerly 2C), magnesium-dependent, alpha isoform	PPM1A			Whitney <i>et al.</i>	221479_s_at	BCL2/adenovirus E1B 19kDa interacting protein 3-like	BNIP3L
		Whitney <i>et al.</i>	204187_at	guanosine mono-phosphate reductase	GMPR			Whitney <i>et al.</i>	221747_at	Homo sapiens cDNA FLJ32766 fis, clone TESTI2001862, mRNA sequence	
		Whitney <i>et al.</i>	204466_s_at	synuclein, alpha (non A4 component of amyloid precursor)	SNCA			Whitney <i>et al.</i>	221748_s_at	Homo sapiens cDNA FLJ32766 fis, clone TESTI2001862, mRNA sequence	
		Whitney <i>et al.</i>	204467_s_at	synuclein, alpha (non A4 component of amyloid precursor)	SNCA			Whitney <i>et al.</i>	221991_at	neurexophilin 3	NXP3
		Whitney <i>et al.</i>	205281_s_at	phosphatidylinositol glycan, class A (paroxysmal nocturnal hemoglobinuria)	PIGA			Whitney <i>et al.</i>	222007_s_at	FK506 binding protein 8, 38kDa	FKBP8
		Whitney <i>et al.</i>	205389_s_at	ankyrin 1, erythrocytic	ANK1		Reticulo- cytes	GSK	211696_x_at	Hemoglobin, Beta	HBB
		Whitney <i>et al.</i>	205390_s_at	ankyrin 1, erythrocytic	ANK1		Red Blood Cells	Affymetrix	216063_at	ESTs, Weakly similar to HBE_HUMAN HEMOGLOBIN EPSILON CHAIN [H.sapiens]	
		Whitney <i>et al.</i>	205391_x_at	ankyrin 1, erythrocytic	ANK1			Affymetrix	204018_x_at	hemoglobin, alpha 1	HBA1
		Whitney <i>et al.</i>	205541_s_at	G1 to S phase transition 2	GSPT2			Affymetrix	209458_x_at	hemoglobin, alpha 1	HBA1
		Whitney <i>et al.</i>	205959_at	matrix metallo-proteinase 13 (collagenase 3)	MMP13			Affymetrix	211699_x_at	hemoglobin, alpha 1	HBA1
		Whitney <i>et al.</i>	206416_at	zinc finger protein 205	ZNF205			Affymetrix	211745_x_at	hemoglobin, alpha 2	HBA2
		Whitney <i>et al.</i>	208632_at	ring finger protein 10	RNF10			Affymetrix	214414_x_at	hemoglobin, alpha 2	HBA2
		Whitney <i>et al.</i>	208691_at	transferrin receptor (p90, CD71)	TFRC			Affymetrix	209116_x_at	hemoglobin, beta	HBB
		Whitney <i>et al.</i>	209193_at	pim-1 oncogene	PIM1			Affymetrix	206834_at	hemoglobin, delta	HBD
		Whitney <i>et al.</i>	209339_at	seven in absentia homolog 2 (Drosophila)	SIAH2			Affymetrix	205919_at	hemoglobin, epsilon 1	HBE1
		Whitney <i>et al.</i>	209869_at	adrenergic, alpha-2A-, receptor	ADRA2A			Affymetrix	204848_x_at	hemoglobin, gamma A	HBG1
		Whitney <i>et al.</i>	209890_at	tetraspan 5	TM4SF9			Affymetrix	204419_x_at	hemoglobin, gamma G	HBG2
		Whitney <i>et al.</i>	210746_s_at	erythrocyte membrane protein band 4.2	EPB42			Affymetrix	213515_x_at	hemoglobin, gamma G	HBG2
		Whitney <i>et al.</i>	211992_at	protein kinase, lysine deficient 1	PRKWNK1			Affymetrix	220807_at	hemoglobin, theta 1	HBQ1
		Whitney <i>et al.</i>	211993_at	protein kinase, lysine deficient 1	PRKWNK1			Affymetrix	206647_at	hemoglobin, zeta	HBZ

## Appendix 2: Probe sets significantly different between Ficoll gradient processed at 8°C and room temperature.

Probe Set Name	SLR (Ficoll 8°C vs Ficoll RT)	Gene Description
217591_at	-0.9376893	Consensus includes gb:BF725121 /FEA=EST /DB_XREF=gi:12041032 /DB_XREF=est:bx12e01.x1 /CLONE=bx12e01 /UG=Hs.272108 ESTs

### Appendix 3: Probe sets significantly different between Ficoll gradient processed after overnight incubation and immediate processing.

Probe Set Name	SLR (O/N vs ASAP)	Gene Description	Gene Symbol	Probe Set Name	SLR (O/N vs ASAP)	Gene Description	Gene Symbol
205898_at	-3.727719	chemokine (C-X3-C motif) receptor 1	CX3CR1	203614_at	-1.080288	KIAA0266 gene product	KIAA0266
219243_at	-2.900807	immunity associated protein 4	HIMAP4	201831_s_at	-1.070218	vesicle docking protein p115	VDP
206978_at	-2.777941	chemokine (C-C motif) receptor 2	CCR2	203080_s_at	-1.05084	bromodomain adjacent to zinc finger domain, 2B	BAZ2B
219777_at	-2.397894	hypothetical protein FLJ22690	FLJ22690	219467_at	-1.049529	hypothetical protein FLJ20125	FLJ20125
209829_at	-2.333454	chromosome 6 open reading frame 32	C6orf32	212513_s_at	-1.048441	pVHL-interacting deubiquitinating enzyme 1	VDU1
205202_at	-2.059072	protein-L-isoaspartate (D-aspartate) O-methyltransferase	PCMT1	205449_at	-1.029415	protein predicted by clone 23627	HSU79266
213102_at	-1.942772	ARP3 actin-related protein 3 homolog (yeast)	ACTR3	202559_x_at	-1.022468	DKFZP547E1010 protein	DKFZP547E1010
221937_at	221937_at	Homo sapiens cDNA FLJ34482 fis, clone HLUNG2004067, mRNA sequence		208986_at	-1.018431	transcription factor 12 (HTF4, helix-loop-helix transcription factors 4)	TCF12
218242_s_at	-1.901728	CGI-85 protein	CGI-85	218196_at	-1.017374	HSPC019 protein	HSPC019
218659_at	-1.813944	KIAA1685 protein FLJ10687	FLJ10687	201054_at	-1.001394	heterogeneous nuclear ribonucleoprotein A0	HNRPA0
202688_at	-1.793458	tumor necrosis factor (ligand) superfamily, member 10	TNFSF10	201098_at	-1.000894	coatamer protein complex, subunit beta 2 (beta prime)	COPB2
203102_s_at	-1.774261	mannosyl (alpha-1,6-)-glycoprotein beta-1,2-N-acetylglucosaminyl transferase	AGMT2	219691_at	-0.998955	hypothetical protein FLJ20073	FLJ20073
212632_at	-1.68373	Homo sapiens clone 24889 mRNA sequence		217724_at	-0.9937942	PAI-1 mRNA-binding protein	PAI-RBP1
218361_at	-1.647367	hypothetical protein FLJ10687	FLJ10687	202564_x_at	-0.981827	ADP-ribosylation factor-like 2	ARL2
201832_s_at	-1.615451	vesicle docking protein p115	VDP	209630_s_at	-0.9774469	Homo sapiens cDNA FLJ38058 fis, clone CTONG2014898, mRNA sequence	
218303_x_at	-1.531388	hypothetical protein LOC51315	LOC51315	212731_at	-0.9739949	Homo sapiens cDNA FLJ37916 fis, clone CTONG1000094, weakly similar to CYCLIN-DEPENDENT KINASE 6 INHIBITOR, mRNA sequence	
201448_at	-1.523018	Homo sapiens cDNA FLJ36425 fis, clone THYMU2011482, mRNA sequence		202771_at	-0.9404259	KIAA0233 gene product	KIAA0233
211784_s_at	-1.496246	Similar to splicing factor, arginine/serine-rich 2 (SC-35) [Homo sapiens], mRNA sequence		212118_at	-0.9365762	ret finger protein	RFP
211257_x_at	-1.488024	NP220 nuclear protein	NP220	201716_at	-0.9348963	sorting nexin 1	SNX1
203275_at	-1.480717	interferon regulatory factor 2	IRF2	40273_at	-0.9343171	D site of albumin promoter (albumin D-box) binding protein	DBP
218614_at	-1.462767	hypothetical protein FLJ10652	FLJ10652	218889_at	-0.9314525	AD24 protein	AD24
204683_at	-1.418423	intercellular adhesion molecule 2	ICAM2	214440_at	-0.8867887	N-acetyltransferase 1 (arylamine N-acetyltransferase)	NAT1
201503_at	-1.380078	Ras-GTPase-activating protein SH3-domain-binding protein	G3BP	212802_s_at	-0.8665841	DKFZP434C212 protein	DKFZP434C212
218230_at	-1.366544	arfaptin 1	HSU52521	208882_s_at	-0.8613311	progesterin induced protein	DD5
212115_at	-1.349615	HN1 like	HN1L	208644_at	-0.8429819	ADP-ribosyltransferase (NAD+; poly (ADP-ribose) polymerase)	ADPRT
211684_s_at	-1.335757	dynein, cytoplasmic, intermediate polypeptide 2	DNCI2	209206_at	-0.8390855	SEC22 vesicle trafficking protein-like 1 (S. cerevisiae)	SEC22L1
201734_at	-1.329125	Homo sapiens mRNA; cDNA DKFZp564I0463 (from clone DKFZp564I0463), mRNA sequence		213188_s_at	-0.8230567	hypothetical protein DKFZp667G2110	DKFZp667G2110
219083_at	-1.290309	hypothetical protein FLJ10539	FLJ10539	204354_at	-0.8201475	protection of telomeres 1	POT1
213573_at	-1.286128	karyopherin (importin) beta 1	KPNB1	200994_at	-0.8110922	RAN binding protein 7	RANBP7
219035_s_at	-1.282815	ring finger protein 34	RNF34	211758_x_at	-0.7928366	ATP binding protein associated with cell differentiation	APACD
203427_at	-1.260008	DKFZP547E2110 protein	DKFZP547E2110	202225_at	-0.7892394	v-crk sarcoma virus CT10 oncogene homolog (avian)	CRK
217727_x_at	-1.245723	vacuolar protein sorting 35 (yeast)	VPS35	203487_s_at	-0.7739426	DKFZP434A043 protein	DKFZP434A043
217986_s_at	-1.242328	bromodomain adjacent to zinc finger domain, 1A	BAZ1A	213246_at	-0.7716036	DKFZP564F1123 protein	DKFZP564F1123
219539_at	-1.239965	gem (nuclear organelle) associated protein 6	GEMIN6	213174_at	-0.7587999	KIAA0227 protein	KIAA0227
201086_x_at	-1.237814	SON DNA binding protein	SON	212905_at	-0.7199875	likely ortholog of mouse variant polyadenylation protein CSTF-64	CSTF2T
216602_s_at	-1.232038	phenylalanine-tRNA synthetase-like	FARSL	200614_at	-0.7020916	clathrin, heavy polypeptide (Hc)	CLTC
204236_at	-1.219567	Friend leukemia virus integration 1	FLI1	200807_s_at	-0.6635235	heat shock 60kDa protein 1 (chaperonin)	HSPD1
201331_s_at	-1.213799	signal transducer and activator of transcription 6, interleukin-4 induced	STAT6	208985_s_at	-0.6628479	eukaryotic translation initiation factor 3, subunit 1 alpha, 35kDa	EIF3S1
217792_at	-1.208914	sorting nexin 5	SNX5	212880_at	-0.6576837	WD repeat domain 7	WDR7
211342_x_at	-1.187546			204994_at	-0.6304609	myxovirus (influenza virus) resistance 2 (mouse)	MX2
209285_s_at	-1.181918	KIAA1105 protein	RAP140	219979_s_at	-0.6289344	hypothetical protein HSPC138	HSPC138
204314_s_at	-1.172422	cAMP responsive element binding protein 1	CREB1	212222_at	-0.5453832	proteasome activator 200 kDa	PA200
218138_at	-1.15711	McKusick-Kaufman syndrome	MKKS	208735_s_at	0.5441049	conserved gene amplified in osteosarcoma	OS4
202808_at	-1.151961	hypothetical protein FLJ20154	FLJ20154	202753_at	0.5738869	KIAA0107 gene product	KIAA0107
202856_s_at	-1.15159	solute carrier family 16 (monocarboxylic acid transporters), member 3	SLC16A3	205281_s_at	0.629927	phosphatidylinositol glycan, class A (paroxysmal nocturnal hemoglobinuria)	PIGA
200901_s_at	-1.113696	mannose-6-phosphate receptor (cation dependent)	M6PR	202646_s_at	0.6623891	NRAS-related gene	D1S155E
202786_at	-1.092648	serine threonine kinase 39 (STE20/SPS1 homolog, yeast)	STK39				
214531_s_at	-1.0892	sorting nexin 1	SNX1				

Probe Set Name	SLR (O/N vs ASAP)	Gene Description	Gene Symbol	Probe Set Name	SLR (O/N vs ASAP)	Gene Description	Gene Symbol
201898_s_at	0.6898327	ubiquitin-conjugating enzyme E2A (RAD6 homolog)	UBE2A	219634_at	1.218582	chondroitin 4-sulfotransferase	C4ST
200668_s_at	0.6968125	ubiquitin-conjugating enzyme E2D 3 (UBC4/5 homolog, yeast)	UBE2D3	214714_at	1.286237	hypothetical protein FLJ12298	FLJ12298
219099_at	0.7328408	chromosome 12 open reading frame 5	C12orf5	217783_s_at	1.287352	yippee protein	CGI-127
206919_at	0.7539121	ELK4, ETS-domain protein (SRF accessory protein 1)	ELK4	208632_at	1.322416	ring finger protein 10	RNF10
200794_x_at	0.7683366	DAZ associated protein 2	DAZAP2	209020_at	1.379156	chromosome 20 open reading frame 111	C20orf111
202467_s_at	0.8326623	thyroid receptor interacting protein 15	TRIP15	213134_x_at	1.443638	BTG family, member 3	BTG3
204180_s_at	0.8382008	zinc finger protein 297B	ZNF297B	200730_s_at	1.469874	protein tyrosine phosphatase type IVA, member 1	PTP4A1
208734_x_at	0.932318	RAB2, member RAS oncogene family	RAB2	89948_at	1.519275	chromosome 20 open reading frame 67	C20orf67
201573_s_at	0.939643	eukaryotic translation termination factor 1	ETF1	213538_at	1.530418	SON DNA binding protein	SON
208720_s_at	0.9544012	RNA-binding region (RNP1, RRM) containing 2	RNPC2	222045_s_at	1.575985	chromosome 20 open reading frame 67	C20orf67
200870_at	0.9803073	unr-interacting protein	UNRIP	221727_at	1.657049	activated RNA polymerase II transcription cofactor 4	PC4
219646_at	1.006808	hypothetical protein FLJ20186	FLJ20186	212227_x_at	1.687728	putative translation initiation factor	SUI1
200669_s_at	1.007893	ubiquitin-conjugating enzyme E2D 3 (UBC4/5 homolog, yeast)	UBE2D3	212130_x_at	1.708675	putative translation initiation factor	SUI1
200779_at	1.010298	activating transcription factor 4 (tax-responsive enhancer element B67)	ATF4	206342_x_at	1.718217	iduronate 2-sulfatase (Hunter syndrome)	IDS
201593_s_at	1.04098	uncharacterized hypothalamus protein HT010	HT010	202021_x_at	1.740566	putative translation initiation factor	SUI1
202657_s_at	1.049994	transcriptional regulator interacting with the PHS-bromodomain 2	TRIP-Br2	211998_at	1.764859	H3 histone, family 3B (H3.3B)	H3F3B
219397_at	1.098921	hypothetical protein FLJ13448	FLJ13448	205214_at	2.005525	serine/threonine kinase 17b (apoptosis-inducing)	STK17B
222035_s_at	1.102513	Homo sapiens cDNA FLJ33067 fis, clone TRACH2000148, weakly similar to POLY(A) POLYMERASE (EC 2.7.7.19), mRNA sequence		201170_s_at	2.063277	basic helix-loop-helix domain containing, class B, 2	BHLHB2
201574_at	1.122025	eukaryotic translation termination factor 1	ETF1	202912_at	2.072646	adrenomedullin	ADM
200740_s_at	1.129051	SMT3 suppressor of mif two 3 homolog 1 (yeast)	SMT3H1	208078_s_at	2.108911	transcription factor 8 (represses interleukin 2 expression)	TCF8
214280_x_at	1.129772	heterogeneous nuclear ribonucleoprotein A1	HNRPA1	202644_s_at	2.119844	tumor necrosis factor, alpha-induced protein 3	TNFAIP3
206055_s_at	1.131847	small nuclear ribonucleoprotein polypeptide A'	SNRPA1	36711_at	2.169307	v-maf musculoaponeurotic fibrosarcoma oncogene homolog F (avian)	MAFF
202130_at	1.139959	sudD suppressor of bimD6 homolog (A. nidulans)	SUDD	222044_at	2.177362	chromosome 20 open reading frame 67	C20orf67
220046_s_at	1.163798	cyclin L ania-6a	LOC57018	204440_at	2.246193	CD83 antigen (activated B lymphocytes, immunoglobulin superfamily)	CD83
209388_at	1.16871	poly(A) polymerase alpha	PAPOLA	204622_x_at	2.33072	nuclear receptor subfamily 4, group A, member 2	NR4A2
218319_at	1.189293	pellino homolog 1 (Drosophila)	PELI1	202643_s_at	2.40323	tumor necrosis factor, alpha-induced protein 3	TNFAIP3
212508_at	1.189535	modulator of apoptosis 1	MOAP1	217739_s_at	2.442733	pre-B-cell colony-enhancing factor	PBEF
219248_at	1.190281	hypothetical protein MGC2454	MGC2454	202497_x_at	2.449612	solute carrier family 2 (facilitated glucose transporter), member 3	SLC2A3

## Appendix 4: Probe sets significantly different between QIAamp, Ficoll and BD-CPT.

Probeset Name	SLR (QIAamp vs Ficoll)	SLR (BD-CPT vs Ficoll)	Gene Description	Gene Symbol	Probeset Name	SLR (QIAamp vs Ficoll)	SLR (BD-CPT vs Ficoll)	Gene Description	Gene Symbol
202379_s_at	-1.476698	-0.1529669	natural killer-tumor recognition sequence	NKTR	211725_s_at	0.6283751	0.1105828	Unknown (protein for MGC:4736) [Homo sapiens], mRNA sequence	
203113_s_at	-1.097693	-0.2963687	eukaryotic translation elongation factor 1 delta (guanine nucleotide exchange protein)	EEF1D	217521_at	0.638143	-0.0508649	histidine ammonia-lyase	HAL
201268_at	-1.071945	-0.106989	non-metastatic cells 2, protein (NM23B) expressed in	NME2	208749_x_at	0.6765584	-0.0713432	flotillin 1	FLOT1
200968_s_at	-0.986304	-0.1296323	peptidylprolyl isomerase B (cyclophilin B)	PPIB	204613_at	0.680847	0.0147458	phospholipase C, gamma 2 (phosphatidylinositol-specific)	PLCG2
213097_s_at	-0.8644949	-0.0813712	zuotin related factor 1	ZRF1	212612_at	0.6812013	0.0401139	REST corepressor	RCOR
202475_at	-0.8205457	-0.1384027	seven transmembrane domain protein	NIFIE14	208864_s_at	0.6824278	-0.1512718	thioredoxin	TXN
219119_at	-0.7989606	-0.0252264	U6 snRNA-associated Sm-like protein LSm8	LSM8	209106_at	0.6902978	-0.1405662	nuclear receptor coactivator 1	NCOA1
200818_at	-0.7602521	-0.1314801	ATP synthase, H+ transporting, mitochondrial F1 complex, O subunit (oligomycin sensitivity conferring protein)	ATP5O	210681_s_at	0.6994534	-0.0880469	ubiquitin specific protease 15	USP15
209024_s_at	-0.7356696	-0.1112955	NS1-associated protein 1	NSAP1	202197_at	0.7008795	-0.0089018	myotubularin related protein 3	MTMR3
221434_s_at	-0.7216138	-0.1607068	hypothetical protein DC50	DC50	50221_at	0.7120405	0.1630856	transcription factor EB	TFEB
203531_at	-0.7174869	-0.0524306	Homo sapiens, clone IMAGE: 4820631, mRNA, mRNA sequence		204022_at	0.7140472	-0.0026795	Nedd4-like ubiquitin-protein ligase	WWP2
214100_x_at	-0.7065398	-0.1340206	Williams-Beuren Syndrome critical region protein 20 copy B	WBSCR20B	205191_at	0.7147076	0.0261586	retinitis pigmentosa 2 (X-linked recessive)	RP2
208765_s_at	-0.663344	0.0121674	heterogeneous nuclear ribonucleoprotein R	HNRPR	207671_s_at	0.7329694	-0.0272441	vitelliform macular dystrophy (Best disease, bestrophin)	VMD2
201406_at	-0.6601327	-0.1699065	ribosomal protein L36A	RPL36A	209418_s_at	0.7426018	0.078733	chromosome 22 open reading frame 19	C22orf19
218467_at	-0.6196879	-0.0669989	hepatocellular carcinoma susceptibility protein	HCCA3	219492_at	0.743073	-0.1872416	cystein-rich hydrophobic domain 2	CHIC2
208894_at	-0.5998287	-0.0213203	major histocompatibility complex, class II, DR alpha	HLA-DRA	212899_at	0.750524	-0.0160893	KIAA1028 protein	KIAA1028
210759_s_at	-0.5828217	-0.0217393	proteasome (prosome, macro-pain) subunit, alpha type, 1	PSMA1	220740_s_at	0.7721849	0.0472574	solute carrier family 12 (potassium/chloride transporters), member 6	SLC12A6
214170_x_at	-0.5778562	-0.1664599	fumarate hydratase	FH	204071_s_at	0.7873029	-0.1114104	tumor protein p53-binding protein	TP53BPL
219817_at	-0.5670612	-0.0026238	apoptosis-related protein PNAS-1	LOC51275	214766_s_at	0.7880417	0.0372514	ELYS transcription factor-like protein TMBS62	ELYS
208764_s_at	-0.5108841	-0.0179839	ATP synthase, H+ transporting, mitochondrial F0 complex, subunit c (subunit 9), isoform 2	ATP5G2	221523_s_at	0.7896639	-0.1174937	Rag D protein	RAGD
217874_at	-0.5080959	-0.1765787	succinate-CoA ligase, GDP-forming, alpha subunit	SUCLG1	206324_s_at	0.7955594	-0.1530728	death-associated protein kinase 2	DAPK2
213315_x_at	-0.5008045	-0.0231798	iduronate 2-sulfatase (Hunter syndrome)	IDS	212756_s_at	0.796398	0.0565871	KIAA0349 protein	KIAA0349
213738_s_at	-0.4305592	-0.0893608	ATP synthase, H+ transporting, mitochondrial F1 complex, alpha subunit, isoform 1, cardiac muscle	ATP5A1	206208_at	0.7965844	0.0333677	carbonic anhydrase IV	CA4
217726_at	-0.3983552	-0.0455651	CGI-120 protein	COPZ1	211742_s_at	0.7968066	-0.0264207	ecotropic viral integration site 2B	EVI2B
203327_at	-0.3809429	-0.0459538	insulin-degrading enzyme	IDE	208092_s_at	0.8126861	0.2115283	hypothetical protein DKFZp566A1524	DKFZP566A1524
201439_at	-0.3321941	-0.0149136	golgi-specific brefeldin A resistance factor 1	GBF1	218902_at	0.8147025	-0.0496693	hypothetical protein FLJ20005	FLJ20005
205240_at	0.3424605	0.0164856	LGN protein	LGN	202651_at	0.8214524	0.0696681	KIAA0205 gene product	KIAA0205
208734_x_at	0.3680876	-0.0452094	RAB2, member RAS oncogene family	RAB2	201925_s_at	0.8305944	-0.1443141	decay accelerating factor for complement (CD55, Cromer blood group system)	DAF
46270_at	0.4650494	0.0149934	ubiquitin associated protein 1	UBAP1	204563_at	0.830831	-0.1472082	selectin L (lymphocyte adhesion molecule 1)	SELL
209004_s_at	0.4785328	-0.1199441	F-box and leucine-rich repeat protein 5	FBXL5	219634_at	0.8322199	-0.1300264	chondroitin 4-sulfotransferase	C4ST
218979_at	0.4966879	-0.0624462	hypothetical protein FLJ12888	FLJ12888	202565_s_at	0.8451234	-0.0311474	supervillin	SVIL
204724_s_at	0.4985419	0.0154829	collagen, type IX, alpha 3	COL9A3	212470_at	0.8507796	0.0802003	sperm associated antigen 9	SPAG9
209571_at	0.4991796	-0.045444	CBF1 interacting corepressor	CIR	217947_at	0.8663042	0.0954559	chemokine-like factor super family 6	CKLFSF6
212441_at	0.5294018	-0.1208997	KIAA0232 gene product	KIAA0232	35974_at	0.8668951	-0.0147712	lymphoid-restricted membrane protein	LRMP
203265_s_at	0.5301785	-0.0818362	mitogen-activated protein kinase kinase 4	MAP2K4	206934_at	0.8735405	0.1814699	signal-regulatory protein beta 1	SIRPB1
211744_s_at	0.5510427	-0.107765	CD58 antigen, (lymphocyte function-associated antigen 3)	CD58	210483_at	0.8801618	-0.0643704	hypothetical protein MGC31957	MGC31957
206278_at	0.5674974	-0.1634812	platelet-activating factor receptor	PTAFR	203097_s_at	0.881301	-0.0215811	PDZ domain containing guanine nucleotide exchange factor(GEF)1	PDZ-GEF1
210087_s_at	0.5710154	0.0502712	myelin protein zero-like 1	MPZL1	209222_s_at	0.8839489	-0.0567949	oxysterol binding protein-like 2	OSBPL2
203693_s_at	0.5774992	-0.1491764	E2F transcription factor 3	E2F3	202149_at	0.8855236	-0.052646	B cell RAG associated protein	GALNAC4S-6ST
					203066_at	0.8865094	-0.085397		13CDNA73
					204072_s_at	0.8992973	-0.1020703	hypothetical protein CG003	ABHD2
					205566_at	0.9136922	0.3497646	abhydrolase domain containing 2	PTEN
					211711_s_at	0.919486	-0.0059534	phosphatase and tensin homolog (mutated in multiple advanced cancers 1)	
					202333_s_at	0.9201429	-0.0578598	ubiquitin-conjugating enzyme E2B (RAD6 homolog)	UBE2B

Probeset Name	SLR (QIAamp vs Ficoll)	SLR (BD-CPT vs Ficoll)	Gene Description	Gene Symbol	Probeset Name	SLR (QIAamp vs Ficoll)	SLR (BD-CPT vs Ficoll)	Gene Description	Gene Symbol
204470_at	0.9300464	-0.0235355	chemokine (C-X-C motif) ligand 1 (melanoma growth stimulating activity, alpha)	CXCL1	217755_at	1.062426	0.1725949	hematological and neurological expressed 1	HN1
221664_s_at	0.9379218	0.0071125	junctional adhesion molecule 1	JAM1	38149_at	1.068574	-0.0658955	KIAA0053 gene product	KIAA0053
201780_s_at	0.9451919	-0.1091368	ring finger protein 13	RNF13	205180_s_at	1.069052	-0.116887	a disintegrin and metalloproteinase domain 8	ADAM8
221058_s_at	0.9459383	-0.0116226	chemokine-like factor 1	CKLF1	208783_s_at	1.070028	-0.1316644	membrane cofactor protein (CD46, trophoblast-lymphocyte cross-reactive antigen)	MCP
201926_s_at	0.9465354	0.0624497	decay accelerating factor for complement (CD55, Cromer blood group system)	DAF	220326_s_at	1.070976	0.0555353	hypothetical protein FLJ10357	FLJ10357
217748_at	0.9476031	0.2493742	CGI-45 protein	CGI-45	201888_s_at	1.072983	0.2532183	interleukin 13 receptor, alpha 1	IL13RA1
221958_s_at	0.9550251	0.0220083	hypothetical protein FLJ23091	FLJ23091	213349_at	1.074471	0.145604	KIAA0779 protein	KIAA0779
201365_at	0.9640425	0.0748998	ornithine decarboxylase antizyme 2	OAZ2	209088_s_at	1.075985	-0.1898895	ubiquitin 1	UBN1
219242_at	0.9649534	-0.0729083	hypothetical protein FLJ13386	FLJ13386	211763_s_at	1.078855	-0.0215295	ubiquitin-conjugating enzyme E2B (RAD6 homolog)	UBE2B
209512_at	0.9695336	0.0715627	hypothetical protein MGC10940	MGC10940	212770_at	1.087788	0.0700011	transducin-like enhancer of split 3 (E(sp1) homolog, Drosophila)	TLE3
204674_at	0.9712913	0.0132317	lymphoid-restricted membrane protein	LRMP	41387_r_at	1.089611	0.1039326	KIAA0346 protein	KIAA0346
211883_x_at	0.9783378	0.1566322	carcinoembryonic antigen-related cell adhesion molecule 1 (biliary glycoprotein)	CEACAM1	219079_at	1.092216	0.1602025	flavohepatoxin b5+b5R	b5&b5R
202200_s_at	0.9836747	-0.0478167	SFRS protein kinase 1	SRPK1	203185_at	1.102138	0.0698298	Ras association (RalGDS/AF-6) domain family 2	RASSF2
203853_s_at	0.9845773	0.0535526	GRB2-associated binding protein 2	GAB2	202266_at	1.10807	-0.0854534	TRAF and TNF receptor-associated protein	TTRAP
218614_at	0.9880802	-0.1824055	hypothetical protein FLJ10652	FLJ10652	32069_at	1.108137	-0.0212075	Nedd4 binding protein 1	N4BP1
208788_at	0.9911945	-0.1963884	homolog of yeast long chain polyunsaturated fatty acid elongation enzyme 2	HELO1	204882_at	1.108567	-0.15488	KIAA0053 gene product	KIAA0053
217492_s_at	1.008636	-0.0062987	phosphatase and tensin homolog (mutated in multiple advanced cancers 1), pseudogene 1	PTENP1	32091_at	1.116053	0.054072	KIAA0446 gene product	KIAA0446
208052_x_at	1.009627	0.1062385	carcinoembryonic antigen-related cell adhesion molecule 3	CEACAM3	204959_at	1.122725	-0.1702298	myeloid cell nuclear differentiation antigen	MNDA
201779_s_at	1.010717	-0.0685344	ring finger protein 13	RNF13	208981_at	1.128113	0.0895555	platelet/endothelial cell adhesion molecule (CD31 antigen)	PECAM1
212769_at	1.012829	0.0173916	transducin-like enhancer of split 3 (E(sp1) homolog, Drosophila)	TLE3	208983_s_at	1.1295	0.125557	platelet/endothelial cell adhesion molecule (CD31 antigen)	PECAM1
203080_s_at	1.019146	0.0317982	bromodomain adjacent to zinc finger domain, 2B	BAZ2B	219748_at	1.129889	-0.0504721	hypothetical protein FLJ13693	FLJ13693
205068_s_at	1.020968	-0.1484258	GTPase regulator associated with focal adhesion kinase pp125(FAK)	GRAF	201244_s_at	1.137635	0.1782559	v-raf-1 murine leukemia viral oncogene homolog 1	RAF1
204053_x_at	1.022107	-0.0114203	phosphatase and tensin homolog (mutated in multiple advanced cancers 1)	PTEN	206643_at	1.138538	-0.0159758	histidine ammonia-lyase	HAL
220476_s_at	1.027279	0.1191757	hypothetical protein LOC55924	LOC55924	202770_s_at	1.147394	0.0491932	cyclin G2	CCNG2
205896_at	1.03083	0.052983	solute carrier family 22 (organic cation transporter), member 4	SLC22A4	220603_s_at	1.150389	0.0230594	hypothetical protein FLJ11175	FLJ11175
206464_at	1.031307	-0.0054966	BMX non-receptor tyrosine kinase	BMX	209081_s_at	1.150456	-0.0263601	collagen, type XVIII, alpha 1	COL18A1
209073_s_at	1.032883	0.1439797	numb homolog (Drosophila)	NUMB	200958_s_at	1.160097	0.0926821	syndecan binding protein (syntenin)	SDCBP
212506_at	1.034628	-0.145456	Type II AF10/CALM fusion protein [Homo sapiens], mRNA sequence		208991_at	1.167167	0.1756555	Homo sapiens cDNA FLJ35646 fis, clone SPLEN2012743, mRNA sequence	
201651_s_at	1.042352	0.0688061	protein kinase C and casein kinase substrate in neurons 2	PACSLIN2	214321_at	1.17295	0.0250445	nephroblastoma overexpressed gene	NOV
213805_at	1.044275	0.1112769	CGI-58 protein	CGI-58	218136_s_at	1.175656	0.2246259	mitochondrial solute carrier protein	MSCP
204669_s_at	1.04495	-0.1182305	ring finger protein 24	RNF24	201941_at	1.175975	0.0238753	carboxypeptidase D	CPD
208488_s_at	1.04534	0.0907656	complement component (3b/4b) receptor 1, including Knops blood group system	CR1	212975_s_at	1.181494	-0.020801	KIAA0870 protein	KIAA0870
209091_s_at	1.047462	0.0894069	SH3-domain GRB2-like endophilin B1	SH3GLB1	213501_at	1.181885	0.1411413	acyl-Coenzyme A oxidase 1, palmitoyl	ACOX1
210101_x_at	1.048459	0.0826452	SH3-domain GRB2-like endophilin B1	SH3GLB1	212496_s_at	1.188305	-0.0062299	KIAA0876 protein	KIAA0876
201858_s_at	1.050258	0.0410784	proteoglycan 1, secretory granule	PRG1	201192_s_at	1.191893	0.0712462	phosphatidylinositol transfer protein	PITPN
					207857_at	1.197577	0.0201034	leukocyte immunoglobulin-like receptor, subfamily A (with TM domain), member 2	LILRA2
					218739_at	1.19865	0.1346218	CGI-58 protein	CGI-58
					211612_s_at	1.198806	0.1291431	interleukin 13 receptor, alpha 1	IL13RA1
					215001_s_at	1.204227	-0.084557	glutamate-ammonia ligase (glutamine synthase)	GLUL
					221485_at	1.212579	-0.0609266	UDP-Gal:betaGlcNAc beta 1, 4-galactosyltransferase, polypeptide 5	B4GALT5
					218023_s_at	1.214382	0.0124866	chromosome 5 open reading frame 6	C5orf6

Probeset Name	SLR (QIAamp vs Ficoll)	SLR (BD-CPT vs Ficoll)	Gene Description	Gene Symbol	Probeset Name	SLR (QIAamp vs Ficoll)	SLR (BD-CPT vs Ficoll)	Gene Description	Gene Symbol
221484_at	1.218741	-0.0704358	UDP-Gal:betaGlcNAc beta 1, 4- galactosyltransferase, polypeptide 5	B4GALT5	204174_at	1.448684	-0.0932765	arachidonate 5-lipoxygenase-activating protein	ALOX5AP
217167_x_at	1.221322	0.038271	v-ral simian leukemia viral oncogene homolog B (ras related; GTP binding protein)	RALB	218035_s_at	1.454049	0.1324631	RNA-binding protein	FLJ20273
202100_at	1.221477	0.1337984			215990_s_at	1.460265	0.104075	0.104075	B-cell CLL/lymphoma 6 (zinc finger protein 51)
219892_at	1.225771	0.2314088	transmembrane 6 superfamily member 1	TM6SF1	218610_s_at	1.463145	-0.0439787	hypothetical protein FLJ11151	FLJ11151
201943_s_at	1.226652	0.1010529	carboxypeptidase D	CPD	218923_at	1.465809	0.0318911	chitinase, di-N-acetyl-	CTBS
218132_s_at	1.227215	0.0475016	leukocyte receptor cluster (LRC) member 5	LENG5	203042_at	1.473294	-0.0610236	lysosomal-associated membrane protein 2	LAMP2
202897_at	1.230685	0.0623176	protein tyrosine phosphatase, non-receptor type substrate 1	PTPNS1	220990_s_at	1.482433	0.0803764	likely ortholog of rat vacuole membrane protein 1	VMP1
58780_s_at	1.23148	-0.0327297	hypothetical protein FLJ10357	FLJ10357	212860_at	1.48892	-0.0231661	hypothetical protein DKFZp667O2416	DKFZp667-02416
209498_at	1.239577	-0.0633901	carcinoembryonic antigen-related cell adhesion molecule 1 (biliary glycoprotein)	CEACAM1	203021_at	1.490488	-0.0763004	secretory leukocyte protease inhibitor (antileukoproteinase)	SLPI
210845_s_at	1.270838	0.1783522	plasminogen activator, urokinase receptor	PLAUR	219889_at	1.501113	0.2044853	frequently rearranged in advanced T-cell lymphomas	FRAT1
55705_at	1.285417	0.0892721	hypothetical protein BC012775	LOC91300	209137_s_at	1.527319	-0.0122066	ubiquitin specific protease 10	USP10
218924_s_at	1.289098	-0.0974571	chitinase, di-N-acetyl-	CTBS	210904_s_at	1.527511	0.2158499	interleukin 13 receptor, alpha 1	IL13RA1
211924_s_at	1.300904	-0.0242888	plasminogen activator, urokinase receptor	PLAUR	208093_s_at	1.528287	-0.0004121	LIS1-interacting protein NUDEL; endooligopeptidase A	NUDEL
211521_s_at	1.301353	0.3075188	pleckstrin homology, Sec7 and coiled/coil domains 4	PSCD4	210754_s_at	1.538234	0.0523219	v-yes-1 Yamaguchi sarcoma viral related oncogene homolog	LYN
202388_at	1.30819	-0.3664634	regulator of G-protein signalling 2, 24kDa	RGS2	201594_s_at	1.544181	-0.0759565	protein phosphatase 4, regulatory subunit 1	PPP4R1
201412_at	1.309673	0.2219849	low density lipoprotein receptor-related protein 10	LRP10	202990_at	1.545232	-0.1124251	phosphorylase, glycogen; liver (Hers disease, glycogen storage disease type VI)	PYGL
209600_s_at	1.315241	0.0886117	acyl-Coenzyme A oxidase 1, palmitoyl	ACOX1	211317_s_at	1.54997	0.3494385	CASP8 and FADD-like' apoptosis regulator	CFLAR
214784_x_at	1.316766	0.1041788	RAN binding protein 20	RANBP20	221497_x_at	1.554879	-0.1038012	egl nine homolog 1 (C. elegans)	EGLN1
213733_at	1.318887	0.1257599	myosin IIF	MYO1F	201364_s_at	1.563973	0.231241	ornithine decarboxylase antizyme 2	OAZ2
202910_s_at	1.344325	0.1543661	CD97 antigen	CD97	206470_at	1.565708	0.0844799	plexin C1	PLXNC1
220528_at	1.359389	0.0395519	vanin 3	VNN3	206925_at	1.580067	0.349834	sialyltransferase 8D (alpha-2, 8-polysialyltransferase)	SIAT8D
205945_at	1.35994	0.2146405	interleukin 6 receptor	IL6R	219681_s_at	1.610425	0.046414	Rab coupling protein	RCP
212569_at	1.360791	-0.1887283	KIAA0650 protein	KIAA0650	200919_at	1.616666	0.0444438	polyhomeotic-like 2 (Drosophila)	PHC2
205645_at	1.366964	0.0791719	RALBP1 associated Eps domain containing 2	REPS2	213241_at	1.618286	0.1041699	Homo sapiens clone 23785 mRNA sequence	
212830_at	1.367022	0.2310222	EGF-like-domain, multiple 5	EGFL5	203041_s_at	1.620448	-0.0319131	lysosomal-associated membrane protein 2	LAMP2
204308_s_at	1.372442	0.1516192	KIAA0329 gene product	KIAA0329	202498_s_at	1.637791	0.2308296	solute carrier family 2 (facilitated glucose transporter), member 3	SLC2A3
212579_at	1.3746	0.0696041	KIAA0650 protein	KIAA0650	203574_at	1.645317	-0.2439767	nuclear factor, interleukin 3 regulated	NFIL3
221920_s_at	1.374961	0.1044506	mitochondrial solute carrier protein	MSCP	200704_at	1.65055	-0.2510286	LPS-induced TNF-alpha factor	PIG7
206514_s_at	1.381824	0.0569809	cytochrome P450, subfamily IVF, polypeptide 3 (leukotriene B4 omega hydroxylase)	CYP4F3	202499_s_at	1.651636	-0.0667685	solute carrier family 2 (facilitated glucose transporter), member 3	SLC2A3
208485_x_at	1.389417	0.3584483	CASP8 and FADD-like apoptosis regulator	CFLAR	220404_at	1.654119	0.0682489	PRO0611 [Homo sapiens], mRNA sequence	
210452_x_at	1.390024	0.0473757	cytochrome P450, subfamily IVF, polypeptide 2	CYP4F2	202193_at	1.654486	-0.0031913	LIM domain kinase 2	LIMK2
221210_s_at	1.39883	0.0090594	chromosome 1 open reading frame 13	C1orf13	205174_s_at	1.661349	0.045951	glutaminyl-peptide cyclotransferase (glutaminy cyclase)	QPCT
204748_at	1.409033	-0.2449054	prostaglandin-endoperoxide synthase 2 (prostaglandin G/H synthase and cyclooxygenase)	PTGS2	208637_x_at	1.663724	0.1980029	actinin, alpha 1	ACTN1
206584_at	1.414106	-0.0150389	MD-2 protein	MD-2	205227_at	1.675569	0.1557606	interleukin 1 receptor accessory protein	IL1RAP
202146_at	1.422887	-0.0256062	interferon-related developmental regulator 1	IFRD1	208918_s_at	1.678291	0.2639081	NAD kinase	FLJ13052
202626_s_at	1.427146	-0.0393655	v-yes-1 Yamaguchi sarcoma viral related oncogene homolog	LYN	216985_s_at	1.733194	0.2566449	syntaxin 3A	STX3A
201463_s_at	1.427684	0.0480795	transaldolase 1	TALDO1	210387_at	1.742095	0.0856164	H2B histone family, member A	H2BFA
201315_x_at	1.430761	0.1138897	interferon induced trans-membrane protein 2 (1-8D)	IFITM2	209238_at	1.75025	0.0004905	syntaxin 3A	STX3A
203509_at	1.439913	0.066397	soritin-related receptor, L(DLR class) A repeats-containing	SORL1	220005_at	1.750973	0.0727913	G protein-coupled receptor 86	GPR86
204542_at	1.441869	0.1111476	sialyltransferase	STHM	202082_s_at	1.75104	0.1233886	SEC14-like 1 (S. cerevisiae)	SEC14L1
					214455_at	1.757075	0.2123023	H2B histone family, member L	H2BFL
					221803_s_at	1.758424	0.0031225	nuclear receptor binding factor-2	NRBF-2
					205920_at	1.770065	0.2714127	solute carrier family 6 (neurotransmitter transporter, taurine), member 6	SLC6A6

Probeset Name	SLR (QIAamp vs Ficoll)	SLR (BD-CPT vs Ficoll)	Gene Description	Gene Symbol	Probeset Name	SLR (QIAamp vs Ficoll)	SLR (BD-CPT vs Ficoll)	Gene Description	Gene Symbol
205920_at	1.770065	0.2714127	solute carrier family 6 (neurotransmitter transporter, taurine), member 6	SLC6A6	201963_at	2.351458	-0.0257272	fatty-acid-Coenzyme A ligase, long-chain 2	FACL2
210582_s_at	1.793044	-0.0305077	LIM domain kinase 2	LIMK2	200648_s_at	2.494441	0.2325233	glutamate-ammonia ligase (glutamine synthase)	GLUL
203765_at	1.794562	-0.0337623	grancalcin, EF-hand calcium binding protein	GCA	206877_at	2.515199	0.0545164	MAX dimerization protein 1	MAD
207890_s_at	1.811283	0.1270924	matrix metalloproteinase 25	MMP25	211372_s_at	2.518055	0.0881507	interleukin 1 receptor, type II	IL1R2
205147_x_at	1.815573	0.1807517	neutrophil cytosolic factor 4, 40kDa	NCF4	216841_s_at	2.543787	0.2071366	superoxide dismutase 2, mitochondrial	SOD2
210992_x_at	1.822352	-0.0246121	Fc fragment of IgG, low affinity IIa, receptor for (CD32)	FCGR2A	221477_s_at	2.571713	0.3522913	Homo sapiens, clone IMAGE: 4711494, mRNA, mRNA sequence	
201392_s_at	1.838737	0.2219849	insulin-like growth factor 2 receptor	IGF2R	202912_at	2.590767	-0.0410949	adrenomedullin	ADM
202084_s_at	1.840873	0.1369739	SEC14-like 1 (S. cerevisiae)	SEC14L1	221345_at	2.6179	0.0420443	G protein-coupled receptor 43	GPR43
211982_x_at	1.846803	0.220534	RAN binding protein 20	RANBP20	206026_s_at	2.726166	-0.0060166	tumor necrosis factor, alpha-induced protein 6	TNFAIP6
210724_at	1.850034	-0.020005	egf-like module-containing mucin-like receptor 3	EMR3	215223_s_at	2.74766	0.1026998	superoxide dismutase 2, mitochondrial	SOD2
205118_at	1.871279	-0.1606469	formyl peptide receptor 1	FPR1	209395_at	2.773115	0.0053545	chitinase 3-like 1 (cartilage glycoprotein-39)	CHI3L1
201393_s_at	1.87975	0.2134208	insulin-like growth factor 2 receptor	IGF2R	210484_s_at	2.848496	0.0379566	hypothetical protein MGC31957	MGC31957
200706_s_at	1.884082	0.0757226	LPS-induced TNF-alpha factor	PIG7	206025_s_at	2.852009	0.0243686	tumor necrosis factor, alpha-induced protein 6	TNFAIP6
213506_at	1.885288	-0.1366932	coagulation factor II (thrombin) receptor-like 1	F2RL1	209396_s_at	2.888263	0.0137153	chitinase 3-like 1 (cartilage glycoprotein-39)	CHI3L1
222088_s_at	1.913609	0.3087584	glucose transporter 14	SCL2A14	205403_at	2.888734	-0.1045352	interleukin 1 receptor, type II	IL1R2
209179_s_at	1.920432	0.0921937	leukocyte receptor cluster (LRC) member 4	LENG4	203434_s_at	2.909016	0.0077991	membrane metallo-endopeptidase (neutral endopeptidase, enkephalinase, CALLA, CD10)	MME
220945_x_at	1.942643	-0.0144417	hypothetical protein FLJ10298	FLJ10298	202391_at	2.971107	-0.0407475	brain abundant, membrane attached signal protein 1	BASP1
202083_s_at	1.951554	0.1869795	SEC14-like 1 (S. cerevisiae)	SEC14L1	205922_at	2.982492	-0.0432557	vanin 2	VNN2
206471_s_at	1.95886	0.1801821	plexin C1	PLXNC1	205568_at	3.00001	-0.0450553	aquaporin 9	AQP9
210772_at	1.983984	-0.0633144	formyl peptide receptor-like 1	FPRL1	207275_s_at	3.047354	0.181051	fatty-acid-Coenzyme A ligase, long-chain 1	FACL1
217202_s_at	2.004346	0.4654353	neutrophil cytosolic factor 4, 40kDa	NCF4	204006_s_at	3.055085	0.3457746	Fc fragment of IgG, low affinity IIIb, receptor for (CD16)	FCGR3B
207677_s_at	2.011658	-0.053554	complement component 5 receptor 1 (C5a ligand)	C5R1	203936_s_at	3.25805	0.2500442	matrix metalloproteinase 9 (gelatinase B, 92kDa gelatinase, 92kDa type IV collagenase)	MMP9
220088_at	2.024924	-0.1070399	formyl peptide receptor 1 chromosome 1 open reading frame 24	C1orf24	218963_s_at	3.282161	0.0843327	type I intermediate filament cytokeratin	HAIK1
205119_s_at	2.058883	0.0658136	solute carrier family 2 (facilitated glucose transporter), member 3	SLC2A3	206222_at	3.302346	0.091331	tumor necrosis factor receptor superfamily, member 10c, decoy without an intracellular domain	TNFRSF10C
217967_s_at	2.078486	-0.0084939	frequently rearranged in advanced T-cell lymphomas 2	FRAT2	206515_at	3.326912	-0.0007966	cytochrome P450, subfamily IVF polypeptide 3 (leukotriene B4 omega hydroxylase)	CYP4F3
216236_s_at	2.083802	0.1919629	hypothetical protein BC012775 chromosome 1 open reading frame 24	LOC91300	203435_s_at	3.346751	0.1015468	membrane metallo-endopeptidase (neutral endopeptidase, enkephalinase, CALLA, CD10)	MME
209864_at	2.094451	0.1088795	chromosome 1 open reading frame 24	C1orf24	205220_at	3.371456	0.0008193	putative chemokine receptor; GTP-binding protein	HM74
221764_at	2.108657	0.3102477	B-cell CLL/lymphoma 6 (zinc finger protein 51)	BCL6	210119_at	3.377942	-0.0269861	potassium inwardly-rectifying channel, subfamily J, member 15	KCNJ15
217966_s_at	2.123187	-0.049725	potassium inwardly-rectifying channel, subfamily J, member 15	KCNJ15	206522_at	3.406912	0.0246788	maltase-glucoamylase (alpha-glucosidase)	MGAM
203140_at	2.126136	0.1248759	Fc fragment of IgG, low affinity IIa, receptor for (CD32)	FCGR2A	217738_at	3.433083	0.0877125	pre-B-cell colony-enhancing factor	PBEF
211806_s_at	2.157597	0.1574467	Alkaline phosphatase precursor (AA -17 to 507) [Homo sapiens], mRNA sequence		207094_at	3.524474	-0.1869795	interleukin 8 receptor, alpha pre-B-cell colony-enhancing factor	IL8RA
203561_at	2.18812	0.150998	solute carrier family 2 (facilitated glucose transporter), member 3	SLC2A3	217739_s_at	3.707827	-0.0277965	interleukin 8 receptor, beta	IL8RB
215783_s_at	2.191544	0.0340491	colony stimulating factor 2 receptor, beta, low-affinity (granulocyte-macrophage)	CSF2RB	211163_s_at	3.803921	-0.177709	tumor necrosis factor receptor superfamily, member 10c, decoy without an intracellular domain	TNFRSF10C
202497_x_at	2.192449	0.2558469	selenoprotein X, 1 triggering receptor expressed on myeloid cells 1	SEPX1	204007_at	4.240474	0.1199834	Fc fragment of IgG, low affinity IIIa, receptor for (CD16)	FCGR3A
205159_at	2.234998	-0.1416655	fatty-acid-Coenzyme A ligase, long-chain 2	FACL2					
217977_at	2.235318	0.1307962	glutamate-ammonia ligase (glutamine synthase)	GLUL					
219434_at	2.308519	0.0734442	fatty-acid-Coenzyme A ligase, long-chain 2	FACL2					

## Appendix 5: Probe sets significantly different between QIAamp and PAXgene.

Probeset Name	SLR (QIAamp vs PAXgene)	Gene Description	Gene Symbol
201178_at	-2.739499	F-box only protein 7	FBX07
215812_s_at	-2.707031	ESTs, Highly similar to S6AA_HUMAN Sodium- and chloride-dependent creatine transporter 2 (CT2) [H.sapiens]	
201161_s_at	-2.566654	cold shock domain protein A	CSDA
200844_s_at	-2.257423	SET domain, bifurcated 1	SETDB1
201160_s_at	-2.18458	cold shock domain protein A	CSDA
220515_at	-1.914253	low molecular weight dual specificity phosphatase 21	LMWDSP21
216011_at	-1.84626	Homo sapiens, clone IMAGE:4776814, mRNA, mRNA sequence	
219385_at	-1.631347	B lymphocyte activator macrophage expressed	BLAME
221859_at	-1.485993	synaptotagmin XIII	SYT13
203287_at	-1.30464	ladinin 1	LAD1
211736_at	-1.230065	Sp2 transcription factor	SP2
211552_s_at	-1.120583	aldehyde dehydrogenase 4 family, member A1	ALDH4A1
217677_at	-1.093915	pleckstrin homology domain containing, family A (phosphoinositide binding specific) member 2	PLEKHA2
213874_at	-1.066279	serine (or cysteine) proteinase inhibitor, clade A (alpha-1 antiproteinase, antitrypsin), member 4	SERPINA4
205486_at	-1.026765	testis-specific kinase 2	TESK2
220366_at	-0.9936848	epididymal sperm binding protein 1	ELSPBP1
207701_at	-0.9479684	hypothetical protein HSN44A4A	HSN44A4A
214759_at	-0.9466152	Wilms' tumour 1-associating protein	WTAP
216671_x_at	-0.764229	mucin 8, tracheobronchial	MUC8
214406_s_at	-0.6527526	solute carrier family 7 (cationic amino acid transporter, y+ system), member 4	SLC7A4
203452_at	-0.605628	beta-1,3-glucuronyltransferase 3 (glucuronosyltransferase I)	B3GAT3
215347_at	-0.2186629	Homo sapiens cDNA FLJ10265 fis, clone HEMBB1001014, mRNA sequence	
200027_at	0.3298201	asparaginyl-tRNA synthetase	NARS
219762_s_at	1.326458	ribosomal protein L36	RPL36
219539_at	1.723338	gem (nuclear organelle) associated protein 6	GEMIN6
217256_x_at	2.13343		
215089_s_at	2.311769	RNA binding motif protein 10	RBM10
202298_at	2.474429	NADH dehydrogenase (ubiquinone) 1 alpha subcomplex, 1, 75kDa	NDUFA1
217221_x_at	2.563373	RNA binding motif protein 10	RBM10

## Appendix 6: Probe sets significantly different between PAXgene and BD-CPT.

Probeset Name	SLR (PAXgene vs BD-CPT)	Gene Description	Gene Symbol	Probeset Name	SLR (PAXgene vs BD-CPT)	Gene Description	Gene Symbol
200026_at	-5.687186	ribosomal protein L34	RPL34	203113_s_at	-2.541463	eukaryotic translation elongation factor 1 delta (guanine nucleotide exchange protein)	EEF1D
209066_x_at	-5.259851	ubiquinol-cytochrome c reductase binding protein	UQCRB	212042_x_at	-2.54009	ribosomal protein L7	RPL7
205849_s_at	-4.859031	ubiquinol-cytochrome c reductase binding protein	UQCRB	209067_s_at	-2.536148	heterogeneous nuclear ribonucleoprotein D-like	HNRPDL
200888_s_at	-4.650724	ribosomal protein L23	RPL23	206662_at	-2.523872	glutaredoxin (thioltransferase)	GLRX
216834_at	-4.355895	B cell activation gene [Homo sapiens], mRNA sequence		201970_s_at	-2.454484	nuclear autoantigenic sperm protein (histone-binding)	NASP
200082_s_at	-4.273576	ribosomal protein S7	RPS7	200781_s_at	-2.447652	ribosomal protein S15a	RPS15A
200061_s_at	-4.261792	ribosomal protein S24	RPS24	217789_at	-2.435227	sorting nexin 6	SNX6
218007_s_at	-4.142826	ribosomal protein S27-like	RPS27L	204982_at	-2.407974	G protein-coupled receptor kinase-interactor 2	GIT2
200099_s_at	-4.100095			200834_s_at	-2.38275	ribosomal protein S21	RPS21
201406_at	-4.094897	ribosomal protein L36A	RPL36A	201354_s_at	-2.373694	bromodomain adjacent to zinc finger domain, 2A	BAZ2A
212537_x_at	-3.875194	ribosomal protein L17	RPL17	218891_at	-2.325911	hypothetical protein FLJ13114	FLJ13114
212270_x_at	-3.820414	ribosomal protein L17	RPL17	219598_s_at	-2.307392	PTD013 protein	PTD013
201134_x_at	-3.680641	cytochrome c oxidase subunit VIlc	COX7C	213251_at	-2.252709	Homo sapiens mRNA; cDNA DKFZp434C2112 (from clone DKFZp434C2112), mRNA sequence	
213941_x_at	-3.605659	ribosomal protein S7	RPS7	221979_at	-2.247978	Unknown (protein for IMAGE: 4152599) [Homo sapiens], mRNA sequence	
200038_s_at	-3.551291	ribosomal protein L17	RPL17	206461_x_at	-2.19558	metallothionein 1H	MT1H
200963_x_at	-3.507056	ribosomal protein L31	RPL31	213737_x_at	-2.191082	Homo sapiens, clone IMAGE: 4133122, mRNA, mRNA sequence	
212578_x_at	-3.442243	ribosomal protein S17	RPS17	218395_at	-2.171653	hypothetical protein FLJ13433	FLJ13433
209732_at	-3.435405	C-type (calcium dependent, carbohydrate-recognition domain) lectin, superfamily member 2 (activation-induced)	CLECSF2	206500_s_at	-2.146744	chromosome 14 open reading frame 106	C14orf106
210908_s_at	-3.412565	prefoldin 5	PFDN5	212326_at	-2.144161	KIAA0453 protein	KIAA0453
207132_x_at	-3.311724	prefoldin 5	PFDN5	201595_s_at	-2.130178	uncharacterized hypothalamus protein HT010	HT010
201473_at	-3.291127	jun B proto-oncogene	JUNB	218482_at	-2.071929	DC6 protein	DC6
211487_x_at	-3.285982			219261_at	-2.008235	hypothetical protein MGC2718	MGC2718
200093_s_at	-3.181122	histidine triad nucleotide binding protein 1	HINT1	218936_s_at	-2.003032	HSPC128 protein	HSPC128
204621_s_at	-3.082052	nuclear receptor subfamily 4, group A, member 2	NR4A2	218738_s_at	-1.973899	STRIN protein	STRIN
201812_s_at	-3.018121	homolog of Tom7 (S. cerevisiae)	TOM7	211998_at	-1.961085	H3 histone, family 3B (H3.3B)	H3F3B
213687_s_at	-2.97788	ribosomal protein L35a	RPL35A	208805_at	-1.959536	proteasome (prosome, macropain) subunit, alpha type, 6	PSMA6
201754_at	-2.966792	cytochrome c oxidase subunit VIc	COX6C	212036_s_at	-1.939966	pinin, desmosome associated protein	PNN
200705_s_at	-2.962576	eukaryotic translation elongation factor 1 beta 2	EEF1B2	200893_at	-1.90957	splicing factor, arginine/serine-rich 10 (transformer 2 homolog, Drosophila)	SFRS10
216380_x_at	-2.946279			202484_s_at	-1.853657	methyl-CpG binding domain protein 2	MBD2
200002_at	-2.924494	ribosomal protein L35	RPL35	212170_at	-1.835973	RNA binding motif protein 12	RBM12
203821_at	-2.922155	diphtheria toxin receptor (heparin-binding epidermal growth factor-like growth factor)	DTR	201987_at	-1.827564	Homo sapiens cDNA FLJ30332 fis, clone BRACE2007254, mRNA sequence	
205644_s_at	-2.890983	small nuclear ribonucleoprotein polypeptide G	SNRPG	200013_at	-1.801293	ribosomal protein L24	RPL24
201257_x_at	-2.886762	ribosomal protein S3A	RPS3A	201290_at	-1.789671	signal peptidase complex (18kD)	SPC18
212391_x_at	-2.879158	ribosomal protein S3A	RPS3A	208695_s_at	-1.788212	ribosomal protein L39	RPL39
203316_s_at	-2.845505	small nuclear ribonucleoprotein polypeptide E	SNRPE	200025_s_at	-1.76783	ribosomal protein L27	RPL27
200826_at	-2.820967	small nuclear ribonucleoprotein D2 polypeptide 16.5kDa	SNRPD2	205292_s_at	-1.748407	heterogeneous nuclear ribonucleoprotein A2/B1	HNRPA2B1
202428_x_at	-2.808576	diazepam binding inhibitor (GABA receptor modulator, acyl-Coenzyme A binding protein)	DBI	212783_at	-1.738347	retinoblastoma binding protein 6	RBBP6
214709_s_at	-2.797337	kinectin 1 (kinesin receptor)	KTN1	203403_s_at	-1.737523	ring finger protein (C3H2C3 type) 6	RNF6
201485_s_at	-2.793125	reticulocalbin 2, EF-hand calcium binding domain	RCN2	221847_at	-1.725693	proline-rich protein HaellI subfamily 1	PRH1
200717_x_at	-2.793123	ribosomal protein L7	RPL7	212469_at	-1.723378	IDN3 protein	IDN3
215963_x_at	-2.761773	ESTs, Weakly similar to S34195 ribosomal protein L3, cytosolic - human [H.sapiens]		200089_s_at	-1.696379	ribosomal protein L4	RPL4
210180_s_at	-2.75638	splicing factor, arginine/serine-rich 10 (transformer 2 homolog, Drosophila)	SFRS10	221475_s_at	-1.69505	ribosomal protein L15	RPL15
200626_s_at	-2.720634	matrin 3	MATR3	200095_x_at	-1.678852	ESTs, Highly similar to S55918	
200977_s_at	-2.5871	Tax1 (human T-cell leukemia virus type I) binding protein 1	TAX1BP1	201532_at	-1.674048	ribosomal protein S10, cytosolic - human [H.sapiens]	
218654_s_at	-2.576701	mitochondrial ribosomal protein S33	MRPS33			proteasome (prosome, macropain) subunit, alpha type, 3	PSMA3
217915_s_at	-2.566493	chromosome 15 open reading frame 15	C15orf15				

Probeset Name	SLR (PAXgene vs BD-CPT)	Gene Description	Gene Symbol	Probeset Name	SLR (PAXgene vs BD-CPT)	Gene Description	Gene Symbol
203259_s_at	-1.658561	CGI-130 protein	CGI-130	202296_s_at	0.5509788	similar to <i>S. cerevisiae</i> RER1	RER1
201916_s_at	-1.631586	SEC63 protein	SEC63L	216526_x_at	0.7182477	major histocompatibility complex, class I, C	HLA-C
221728_x_at	-1.607339	Homo sapiens cDNA FLJ30298 fis, clone BRACE2003172, mRNA sequence		207826_s_at	0.7685451	inhibitor of DNA binding 3, dominant negative helix-loop-helix protein	ID3
201597_at	-1.606136	cytochrome c oxidase subunit VIIa polypeptide 2 (liver)	COX7A2	218941_at	0.8449928	F-box and WD-40 domain protein 2	FBXW2
200050_at	-1.599699	zinc finger protein 146	ZNF146	206975_at	0.905318	lymphotoxin alpha (TNF superfamily, member 1)	LTA
217828_at	-1.587893	hypothetical protein FLJ13213	FLJ13213	216385_at	0.9400882	Docking protein 1-like protein [Homo sapiens], mRNA sequence	
208804_s_at	-1.559257	Homo sapiens mRNA; cDNA DKFZp564J223 (from clone DKFZp564J223), mRNA sequence		210168_at	0.9878972	complement component 6	C6
220046_s_at	-1.550481	cyclin L ania-6a	LOC57018	200695_at	0.9915233	protein phosphatase 2 (formerly 2A), regulatory subunit A (PR 65), alpha isoform	PPP2R1A
211185_s_at	-1.504997	hypothetical protein FLJ14753	FLJ14753	214366_s_at	1.021459	arachidonate 5-lipoxygenase	ALOX5
202001_s_at	-1.504834	NADH dehydrogenase (ubiquinone) 1 alpha subcomplex, 6, 14kDa	NDUFA6	202665_s_at	1.050521	Wiskott-Aldrich syndrome protein interacting protein DKFZP434J154 protein	WASPIP
208746_x_at	-1.502456	ATP synthase, H+ transporting, mitochondrial F0 complex, subunit g	ATP5L	204710_s_at	1.085455		
201368_at	-1.500487	zinc finger protein 36, C3H type-like 2	ZFP36L2	DKFZP434J154			
210453_x_at	-1.497817	ATP synthase, H+ transporting, mitochondrial F0 complex, subunit g	ATP5L	221984_s_at	1.152439	hypothetical protein MGC3035	MGC3035
213151_s_at	-1.485518	CDC10 cell division cycle 10 homolog ( <i>S. cerevisiae</i> )	CDC10	216835_s_at	1.227374	docking protein 1, 62kDa (downstream of tyrosine kinase 1)	DOK1
202322_s_at	-1.467496	geranylgeranyl diphosphate synthase 1	GGPS1	203194_s_at	1.254111	nucleoporin 98kDa	NUP98
200007_at	-1.462908	signal recognition particle 14kDa (homologous Alu RNA binding protein)	SRP14	200803_s_at	1.299656	testis enhanced gene transcript (BAX inhibitor 1)	TEGT
201652_at	-1.440749	COP9 constitutive photomorphogenic homolog subunit 5 ( <i>Arabidopsis</i> )	COPS5	206672_at	1.329247	aquaporin 2 (collecting duct)	AQP2
201170_s_at	-1.341914	basic helix-loop-helix domain containing, class B, 2	BHLHB2	205030_at	1.419243	fatty acid binding protein 7, brain	FABP7
220044_x_at	-1.334343	cisplatin resistance-associated overexpressed protein	LUC7A	221874_at	1.423178	KIAA1324 protein	KIAA1324
204224_s_at	-1.282801	GTP cyclohydrolase 1 (dopa-responsive dystonia)	GCH1	222381_at	1.454074	ESTs, Weakly similar to PRPP_HUMAN SALIVARY PROLINE-RICH PROTEIN II-1 [H.sapiens]	
200009_at	-1.258467	GDP dissociation inhibitor 2	GDII2	211691_x_at	1.479657	Ornithine decarboxylase antizyme 4 [Homo sapiens], mRNA sequence	
212637_s_at	-1.249289	VW domain-containing protein 1	WWP1	201957_at	1.483485	protein phosphatase 1, regulatory (inhibitor) subunit 12B	PPP1R12B
204528_s_at	-1.243751	nucleosome assembly protein 1-like 1	NAP1L1	210399_x_at	1.520843	fucosyltransferase 6 (alpha (1,3) fucosyltransferase)	FUT6
201962_s_at	-1.212635	hypothetical SBBI03 protein	SBB103	218659_at	1.529909	KIAA1685 protein	FLJ10898
209143_s_at	-1.17521	chloride channel, nucleotide-sensitive, 1A	CLNS1A	202845_s_at	1.563786	ralA binding protein 1	RALBP1
201979_s_at	-1.09402	protein phosphatase 5, catalytic subunit	PPP5C	220283_at	1.571846	hypothetical protein FLJ13840	FLJ13840
218233_s_at	-1.081364	chromosome 6 open reading frame 49	C6orf49	221962_s_at	1.58897	ubiquitin-conjugating enzyme E2H (UBC8 homolog, yeast)	UBE2H
200593_s_at	-1.076199	heterogeneous nuclear ribonucleoprotein U (scaffold attachment factor A)	HNRPU	208110_x_at	1.653099	hypothetical protein TCBAP0758	TCBAP0758
204571_x_at	-0.9489658	protein (peptidyl-prolyl cis/trans isomerase) NIMA-interacting, 4 (parvulin)	PIN4	201350_at	1.688758	flotillin 2	FLOT2
212301_at	-0.948333	KIAA0252 protein	KIAA0252	221063_x_at	1.746133	hypothetical protein FLJ12565	FLJ12565
212056_at	-0.9267216	KIAA0182 protein	KIAA0182	208399_s_at	1.814455	endothelin 3	EDN3
221481_x_at	-0.922991	heterogeneous nuclear ribonucleoprotein D (AU-rich element RNA binding protein 1, 37kDa)	HNRPD	220467_at	1.849836	hypothetical protein FLJ21272	FLJ21272
201990_s_at	-0.8928844	cAMP responsive element binding protein-like 2	CREBL2	210210_at	1.875723	myelin protein zero-like 1	MPZL1
206621_s_at	-0.7597733	Williams-Beuren syndrome chromosome region 1	WBSCR1	213602_s_at	1.934863	matrix metalloproteinase 11 (stromelysin 3)	MMP11
211788_s_at	0.2183863	three prime repair exonuclease 2	TREX2	209018_s_at	2.015434	PTEN induced putative kinase 1	PINK1
207685_at	0.2749432	crystallin, beta B3	CRYBB3	216183_at	2.046485	Hypothetical protein [Homo sapiens], mRNA sequence	
205918_at	0.4024484	solute carrier family 4, anion exchanger, member 3	SLC4A3	220722_s_at	2.089928	solute carrier family 5 (choline transporter), member 7	SLC5A7
				201315_x_at	2.099153	interferon induced transmembrane protein 2 (1-8D)	IFITM2
				221447_s_at	2.154766	glycosyltransferase	LOC83468
				222357_at	2.167585	Homo sapiens, clone IMAGE: 4291354, mRNA, mRNA sequence	
				207252_at	2.16826	inactivation escape 1	INE1
				221479_s_at	2.213265	BCL2/adenovirus E1B 19kDa interacting protein 3-like	BNIP3L
				204555_s_at	2.249689	protein phosphatase 1, regulatory subunit 3D	PPP1R3D
				212055_at	2.269707	DKFZP586M1523 protein	DKFZP586-M1523

Probeset Name	SLR (PAXgene vs BD-CPT)	Gene Description	Gene Symbol	Probeset Name	SLR (PAXgene vs BD-CPT)	Gene Description	Gene Symbol
221013_s_at	2.395719	apolipoprotein L, 2	APOL2	202387_at	3.187397	BCL2-associated athanogene	BAG1
211546_x_at	2.472878	synuclein, alpha (non A4 component of amyloid precursor)	SNCA	201178_at	3.214718	F-box only protein 7	FBXO7
213768_s_at	2.5937	achaete-scute complex-like 1 (Drosophila)	ASCL1	213843_x_at	3.22379	solute carrier family 6 (neurotransmitter transporter, creatine), member 8	SLC6A8
204826_at	2.612615	cyclin F	CCNF	217748_at	3.336225	CGI-45 protein	CGI-45
55705_at	2.642007	hypothetical protein BC012775	LOC91300	201161_s_at	3.426484	cold shock domain protein A	CSDA
204542_at	2.643964	sialyltransferase	STHM	218864_at	3.703149	tensin	TNS
201912_s_at	2.65028	G1 to S phase transition 1	GSPT1	202947_s_at	3.895885	glycophorin C (Gerbich blood group)	GYPC
211820_x_at	2.69462	glycophorin A (includes MN blood group)	GYPA	205220_at	3.952434	putative chemokine receptor; GTP-binding protein	HM74
221674_s_at	2.69788	chordin	CHRD	209396_s_at	4.100931	chitinase 3-like 1 (cartilage glycoprotein-39)	CHI3L1
220937_s_at	2.741562	sialyltransferase 7D ((alpha-N-acetylneuraminy-2,3-beta-galactosyl-1,3)-N-acetyl galactosaminide	SIAT7D	218136_s_at	4.240891	mitochondrial solute carrier protein	MSCP
209179_s_at	2.778334	alpha-2,6-sialyltransferase) leukocyte receptor cluster (LRC) member 4	LENG4	221345_at	4.719292	G protein-coupled receptor 43	GPR43
221764_at	2.982583	hypothetical protein BC012775	LOC91300	217202_s_at	4.784796	membrane metallo-endopeptidase (neutral endopeptidase, enkephalinase, CALLA, CD10)	MME
221748_s_at	2.989036	Homo sapiens cDNA FLJ32766 fis, clone TESTI2001862, mRNA sequence		203435_s_at	4.999364	chitinase 3-like 1 (cartilage glycoprotein-39)	CHI3L1
220404_at	2.996874	PRO0611 [Homo sapiens], mRNA sequence		209395_at	5.081478	solute carrier family 6 (neurotransmitter transporter, creatine), member 8	SLC6A8
211821_x_at	3.042027	glycophorin A (includes MN blood group)	GYPA	202219_at	5.087781	Fc fragment of IgG, low affinity IIIa, receptor for (CD16)	FCGR3A
221824_s_at	3.060475	hypothetical protein MGC26766	MGC26766	204007_at	5.090703	interleukin 8 receptor, alpha	IL8RA
207890_s_at	3.155642	matrix metalloproteinase 25	MMP25	207094_at	5.522098	erythrocyte membrane protein band 4.2	EPB42
206222_at	3.159306	tumor necrosis factor receptor superfamily, member 10c, decoy without an intracellular domain	TNFRSF10C	210746_s_at	5.626492	cytochrome b5 outer mitochondrial membrane precursor	CYB5-M
207827_x_at	3.166961	synuclein, alpha (non A4 component of amyloid precursor)	SNCA	211560_s_at	7.765874		

**AFFYMETRIX, INC.**

3380 Central Expressway  
Santa Clara, CA 95051 USA  
Tel: 1-888-DNA-CHIP (1-888-362-2447)  
Fax: 1-408-731-5441  
sales@affymetrix.com  
support@affymetrix.com

**AFFYMETRIX UK Ltd**

Voyager, Mercury Park,  
Wycombe Lane, Wooburn Green,  
High Wycombe HP10 0HH  
United Kingdom  
Tel: +44 (0) 1628 552550  
Fax: +44 (0) 1628 552585  
saleseurope@affymetrix.com  
supporteurope@affymetrix.com




**AFFYMETRIX JAPAN K.K.**

Mita NN Bldg., 16 F  
4-1-23 Shiba, Minato-ku,  
Tokyo 108-0014 Japan  
Tel: +81-(0)3-5730-8200  
Fax: +81-(0)3-5730-8201  
salesjapan@affymetrix.com  
supportjapan@affymetrix.com

[www.affymetrix.com](http://www.affymetrix.com)

**For research use only.  
Not for use in diagnostic procedures.**

Part No. 701406 Rev. 1

©2003 Affymetrix, Inc. All rights reserved. Affymetrix®, GeneChip®, ®, ®, ®, HuSNP®, Jaguar™, EASI™, MicroDB™, GenFlex®, CustomExpress™, CustomSeq™, NetAffx™, "Tools to take you as far as your vision™", and "The Way Ahead™" are trademarks owned or used by Affymetrix, Inc. Array products may be covered by one or more of the following patents and/or sold under license from Oxford Gene Technology: U.S. Patent Nos. 5,445,934; 5,744,305; 6,261,776; 6,291,183; 5,700,637; 5,945,334; 6,346,413; and 6,399,365; and EP 619 321; 373 203 and other U.S. or foreign patents.